Journal of Geophysical Research: Solid Earth

RESEARCH ARTICLE
10.1029/2018JB015743

Key Points:
- Ground motions of interface earthquakes are depth dependent
- Strong ground motions vary laterally on the Japan subduction interface
- Spatial and temporal variability of ground motion can be used to identify permanent and transient features of the subduction interface

Supporting Information:
- Supporting Information S1

Correspondence to:
J. Piña-Valdés,
jesus.pina-valdes@univ-grenoble-alpes.fr

Citation:
Piña-Valdés, J., Socquet, A., & Cotton, F. (2018). Insights on the Japanese subduction megathrust properties from depth and lateral variability of observed ground motions. *Journal of Geophysical Research: Solid Earth*, *123*. https://doi.org/10.1029/2018JB015743

Received 7 MAR 2018
Accepted 28 SEP 2018
Accepted article online 1 OCT 2018

Insights on the Japanese Subduction Megathrust Properties From Depth and Lateral Variability of Observed Ground Motions

J. Piña-Valdés[1], A. Socquet[1], and F. Cotton[2,3]

[1]University Grenoble Alpes, University Savoie Mont Blanc, CNRS, IRD, IFSTTAR, ISTerre, Grenoble, France, [2]Helmholtz Centre Potsdam, GFZ German Research Centre for Geosciences, Postdam, Germany, [3]Institute for Earth and Environmental Sciences, University of Potsdam, Postdam, Germany

Abstract Two ground motion prediction equation models for subduction zones have been tested using a public ground motion database of the KiK-net records obtained by automated processing protocols (Dawood et al., 2016, https://doi.org/10.1193/071214EQS106). The database contains records of more than 700 interface earthquakes that occurred on the Japan subduction between 1998 and 2012. The Zhao et al. (2006, https://doi.org/10.1785/0120050122) ground motion prediction equation was shown to be the best suited model for the region. It was then used as backbone to analyze the variability of ground motion records. The residuals between observed and predicted ground motions have been analyzed to study the spatial variation of the earthquakes' ground motion frequency content on the Japan megathrust. This analysis revealed a depth dependency of generated ground motions consistent with the downdip segmentation proposed for subduction interfaces (Lay et al., 2012, https://doi.org/10.1029/2011JB009133), a regional ground motion dependency that may be related with lateral variations of the mechanical properties of the subduction interface and a high-frequency radiations drop in the earthquake sequence that preceded the Tohoku-Oki earthquake M_w 9.0. The regional ground motion dependency suggests the existence of different domains along trench of the Japan subduction megathrust that control the ground motions and the wave radiation patterns of interface earthquakes. The location of their boundaries is consistent with the extension of the rupture of the 2011 Tohoku-Oki earthquake, with pre-Tohoku interseismic coupling, and with the free air gravity anomalies.

1. Introduction

The impact of factors such as temperature, pressure, pore fluids, properties and type of sediments, roughness, and fault geometry on the frictional sliding behavior of the subduction interface has been largely discussed (e.g., Hyndman & Wang, 1993; Lay & Bilek, 2007; Marone & Scholz, 1988; Scholz, 1998; Wang & He, 2008). Those parameters can vary significantly along and across subduction zones generating lateral and depth variations of the interface frictional properties (Byrne et al., 1988; Heuret et al., 2011; Hyndman et al., 1997). Indeed, the assent between geological, geodetic, and seismological observations suggests that large megathrust ruptures and their associated slip distributions are related with persistent features that laterally segment the subduction interface (e.g., Béjar-Pizarro et al., 2010; Jara-Munoz et al., 2015; Kodaira et al., 2006; Loveless & Meade, 2010; Moreno et al., 2012; Yamanaka & Kikuchi, 2004). In addition, strong ground motions and teleseismic broadband observations of megathrust ruptures have revealed a depth-frequency dependence of large interface ruptures (Irikura & Kurahashi, 2011; Koper et al., 2011, 2012) that suggests a depth segmentation of the subduction interface frictional behavior, which may impact on the earthquake ground motion generation (Lay et al., 2012).

The surface ground motions are generated by the seismic waves radiated from the source. They are affected by magnitude scaling, rupture directivity, geometrical spreading, attenuation, site amplification, and topographical effects (e.g., Aki, 1967, 1993; Archuleta & Hartzell, 1981; Boore, 1972; Bouchon et al., 1996; Sanchez-Sesma, 1987; Somerville, 2003) that render a comparison between events difficult. These difficulties can be overcome using modern empirical models of ground motions as the ground motion prediction equations (GMPEs).

GMPEs are models that implicitly consider the source, path, and site effects to predict the earthquake ground motions at a given distance from the source, through the prediction of the earthquake response spectra. This

means that GMPEs are not able to predict the ground motions time history but the maximum response of an oscillator of a single degree of freedom to an earthquake over a range of its fundamental period or its fundamental oscillation frequencies.

Usually, the simplified functional forms of the GMPE models are described by equation (1):

$$\mathrm{Log}(Y) = f_{\mathrm{source}}(M, F, Z, \ldots) + f_{\mathrm{path}}(R, M, ..) + f_{\mathrm{site}}(v_{S30}, \ldots) + \varepsilon\sigma \quad (1)$$

on which Y corresponds to the predicted ground motion measure at a given period. The f_{source} term corresponds to a source function that scales the predicted ground motion by magnitude (M) and type of faulting (F), and it can incorporate additional parameters of the source such as the depth (Z). The f_{path} term corresponds to a path function that considers the attenuation by anelastic decay and geometrical spreading and usually is described with variables such as the magnitude and the site to source distance (R). The f_{site} term is a site amplification function that is usually described based on the average shear wave velocities of the top 30 m (v_{S30}) or by the soil type classification of the site. Finally, the term $\varepsilon\sigma$ corresponds to the variability of the ground motions that are log-normally distributed with an average of 0 and a standard deviation equal to σ.

Since the GMPEs correspond to empirical models, they incorporate some of the site, path, and source effects that affect the earthquake ground motions. Therefore, the residuals between the observed ground motions and those predicted by the GMPEs should come from the unmodeled effects of site, source, and propagation that are not able to be captured by simple parameters such as the magnitude, rupture distance, or V_{s30}. Their provenance can be identified disaggregating the residuals (Abrahamson & Youngs, 1992; Al Atik et al., 2010; Baltay et al., 2017; Strasser et al., 2009). GMPE models can therefore be used as *backbones* to study the variations and uncertainties of ground motions generated by different earthquake sources, which may reflect spatial variations of the frictional properties of the subduction interface (Piña-Valdés et al., 2018; Socquet et al., 2017).

In recent years, the requirement of strong ground motion records of large earthquakes for seismic hazard analysis has promoted the development of ground motion sensors as well as the exponential growth of the networks. This has generated a huge quantity of high-quality strong motion records of low and moderate moment magnitude (M_{w}) earthquakes. The impressive development of Japanese strong-motion networks (Aoi et al., 2004; Fujiwara et al., 2004) has given the opportunity to develop large and homogeneously processed data set of subduction earthquakes records (Dawood et al., 2016), which provide a good opportunity to use GMPEs as backbone to study the variability of strong ground motion.

2. Tectonic Context of Japanese Subduction Zone

Japan is located in a complex tectonic setting dominated by two subduction zones (Figure 1a): the Pacific Plate (PAC) and the Philippine Sea Plate (PHS) plunge at 80 and 60 mm/year, respectively, below mainland Japan (DeMets, 1992; DeMets et al., 1990), generating an intense seismic activity and associated seismic hazard. Most of the released seismic energy of the region is related to the subduction process and associated large earthquakes. The largest instrumental earthquake in Japan was the 2011 Tohoku-Oki M_{w} 9.0 megathrust earthquake offshore Honshu. Smaller, but still large, earthquakes occurred on the Nankai subduction interface and in the Kuril trench (e.g., 1944 Tonankai earthquake M_{w} 8.1, 1946 Nankai earthquake M_{w} 8.3, and 2003 Tokachi-Oki earthquake M_{w} 8.1).

The rupture extension of large earthquakes on the PHS interface subduction suggests its lateral segmentation along the Nankai Trough, which seems to be controlled by the geometry of the subducting slab and the presence of seamounts on the oceanic plate, which may act as barriers during the seismic ruptures propagation (e.g., Ando, 1975; Cummins et al., 2002; Kodaira et al., 2006). Similarly, persistent geodetic and seismic segmentation has been observed on the PAC subduction interface, notably at the bend that connects the Japan and the Kuril trenches (e.g., Hashimoto et al., 2009; Tanioka et al., 1997; Yagi, 2004; Yamanaka & Kikuchi, 2004). The presence of this geometrical complexity at the subduction contact may modify the mechanical properties that control the seismic behavior of the subduction interface. Geometrical barriers are generally attributed to the subduction of structures carried by the subducting plate (e.g., oceanic ridges, tear in the oceanic plate, and seamounts; Kodaira et al., 2002, 2006; Tanioka et al., 1997; Wang & Bilek, 2011), but structures in the overriding plate may also influence lateral variations of the megathrust properties. Song and

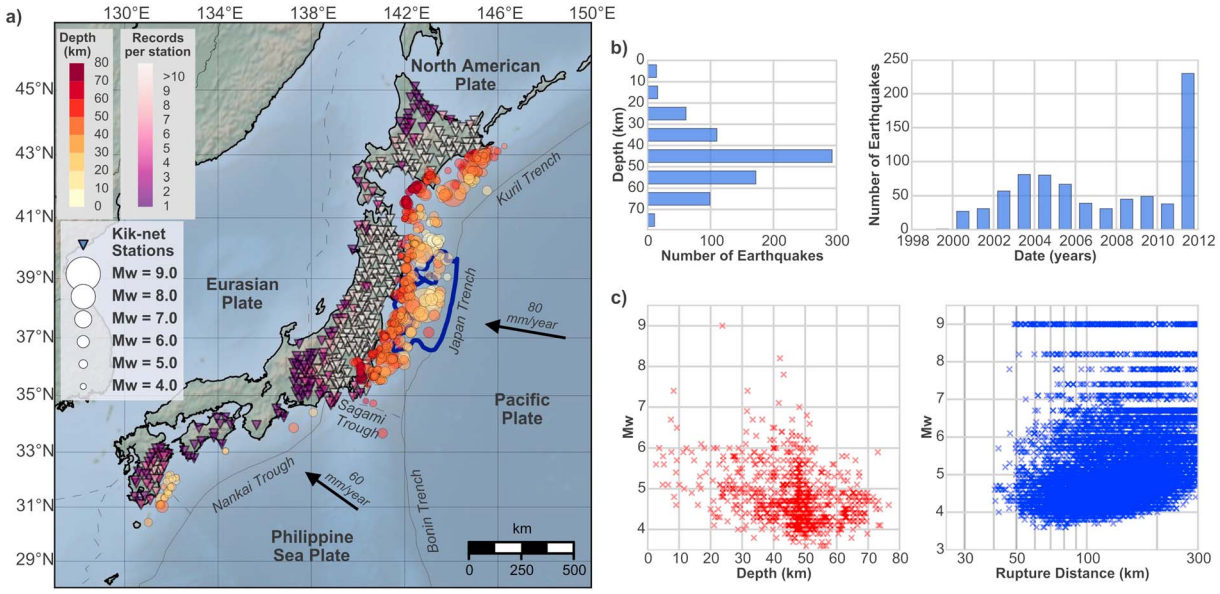

Figure 1. (a) Plate boundaries and tectonic plates around Japan (Bird, 2003). The gray lines show the boundaries of the tectonic plates (continuous lines represent the subduction boundaries). The blue contour represents the rupture of 2011 Tohoku-Oki earthquake M_w 9.0 (Hooper et al., 2013). The circles show the spatial distribution of the interface seismicity with usable strong motion records contained in the Dawood et al. (2016) database. Colors indicate the epicentral depth, and the circle size represents the moment magnitude. The inverted triangles show the location of the KiK-net stations that registered usable records for subduction interface earthquakes, color coded by the number of usable records at each station. (b) Depth and time distribution of the Japan Trench interface seismicity contained in the Dawood et al. (2016) database. Most of the seismicity is concentrated between 30- and 60-km depths, and no interface seismicity is observed below 80-km depth. The peak of seismicity in the year 2011 is related to the 2011 Tohoku-Oki M_w 9.0 earthquake. (c) Distribution of the magnitude of the Japan Trench interface seismicity contained in the Dawood et al. (2016) database as a function of depth and distance to the rupture. Note that the seismicity of low magnitude ($M_w \leq 5.0$) is located between 20- and 80-km depths, with a strong concentration around 50-km depth.

Simons (2003) have shown that the seismogenic behavior in subduction zones (i.e., stick-slip or stable sliding) is strongly correlated with large gravity variations, suggesting that the seismogenic segmentation in a given subduction zone is stationary and linked to the geological structure and topography of the forearc. Patches of the subduction interface that show strong interseismic coupling as well as past earthquakes ruptures indeed seem to correlate with subsiding fore-arc basins associated with tectonic features in the upper plate (Loveless & Meade, 2010; Wells et al., 2003).

The downdip variability on the slip behavior has also been observed by geodetic and seismologic data along the subduction interfaces. In Japan, deep nonvolcanic tremors and associated slow slip events (SSE) occur offshore Nankai on the PHS subduction interface between 35- and 45-km depths (Obara, 2002). Those tremors and SSE may be related to the geothermal gradient and to the presence of fluids along the subduction interface (Ito et al., 2007). Further north, offshore Honshu, nonvolcanic tremors are absent but geodetic observations showed decade-scale transient variations of the slip rate between 30- and 70-km depths on the PAC subduction interface before the rupture of 2011 Tohoku-Oki earthquake (Mavrommatis et al., 2015; Yokota & Koketsu, 2015). Seismological studies (e.g., ground motions measured by local accelerometric networks; e.g. Ide et al., 2011; and backprojection of the teleseismic waves at different frequencies; Kiser & Ishii, 2012; Satriano et al., 2014) showed that the frequency patterns of the energy radiated by the Tohoku earthquake varied with depth (Koper et al., 2011; Lay et al., 2012).

These different observations suggest that the mechanical properties of Japan megathrust vary, both downdip and along strike. Some observations (such as the extent of some large seismic ruptures or the spatial pattern of interseismic coupling) correlate with persistent features (e.g., gravity anomalies, topography, and offshore basins; Song & Simons, 2003; Wells et al., 2003). Instead, other observations are rather characterized by transient behaviors (e.g., transient slip of the deeper part of the seismogenic interface during the decade preceding Tohoku-Oki earthquake and temporal variations of the interseismic coupling; Loveless & Meade, 2016). This suggests that persistent and transient variations of the frictional behavior of the subduction megathrust exist. However, the physical parameters that control the variability of the subduction interface

properties, such as the distribution of unstable patches versus metastable areas, as well their relations with the roughness and the friction, are still not well understood.

The earthquake ground motions have shown to be related with the stress drop variability and the rupture velocity (Bindi et al., 2007, 2017; Causse & Song, 2015; Cotton et al., 2013; Courboulex et al., 2016; Oth et al., 2017). Also, rock experiments and observations on repeated earthquakes have shown that the stress drop is related to the generation of seismic waves of high frequency and is controlled by physical parameters such as faults healing and their frictional heterogeneity (namely, healing rate, healing time, healing heterogeneity, loading rate, pressure, temperature, and mineralogy; Marone, 1998; McLaskey et al., 2012). Therefore, the frequency content of interface earthquakes seems to be representative of the roughness of the subduction interface. The spatial and temporal variation of earthquakes' ground motion frequency content may therefore be used to map the spatial variability of the subduction interface frictional properties and then compare it with independent observations of long-lasting and transient features along the Japan subduction.

Since the selected data set is dense on the Pacific Plate subduction offshore Hokkaido and offshore Honshu, including the region struck by the 2011 Tohoku-Oki earthquake M_w 9.0 where persistent and transient signals have been described, this work is particularly focused on those areas.

3. Interface Ground Motion Database

The KiK-net is a high-quality seismological strong motion network with more than 650 stations deployed along Japan. All stations of this network are composed of two ground motion seismographs, one located in a borehole and the second one at the surface (Aoi et al., 2004; Fujiwara et al., 2004). Since its installation, this network has generated a huge amount of seismic ground acceleration records.

The recent implementation of an automated protocol to process KiK-net's ground acceleration records, as well as metadata collection from the F-net catalog by Dawood et al. (2016), allowed the generation of a large database of homogeneously processed records of more than 3,200 earthquakes of $M_w \geq 3.5$, classified by type (Intraslab/interface), recorded between January 1997 and December 2011. This database contains the response spectra of 873 interface earthquakes distributed along the Japan Trench and the Nankai Trough (Figure 1). This number is large compared to the number of subduction earthquakes used to calibrate the most recent subduction GMPE's. For example, the Zhao et al. (2006) and Abrahamson et al. (2016) models are respectively developed with databases of 269 and 106 earthquakes, including intraslab and interface events. Such large number gives the opportunity to analyze the regional and temporal variations, which are described below.

Taking into account the standard validity range for the rupture distance of the GMPEs, only the horizontal surface records of the database with distance to the rupture smaller than 300 km have been considered. The resulting strong motion database contains more than 12,000 records with rupture distances between 40 and 300 km, which come from 747 interface earthquakes of moment magnitude between 3.6 and 9.0. This catalog includes earthquakes that occurred between 2000 and 2011; almost a third of the earthquakes of the catalog occurred during the year 2011 (Figure 1b). V_{s30} has been measured at all sites, which helps to better take into account the amplifications of soil upper layers.

To avoid bias in the GMPE residual analysis, the records of earthquakes with less than four stations have been removed. Finally, the resulting catalog contains 649 interface earthquakes distributed mainly along the Japan Trench offshore Honshu and Hokkaido (Figure 1a).

The response spectra contained in our selection of the Dawood et al. (2016) database have been validated by picking random records and comparing them with manually processed response spectra from KiK-net records. This manual processing was performed following the guidelines and recommendations of the COSMOS strong motion record workshop (Boore & Bommer, 2005). The instrument offset was removed from the acceleration time series applying a baseline correction. Then, the signal was tapered and zeros were padded at the beginning and the end of the waveform (Akkar et al., 2014). Finally, the acceleration response spectrum was calculated with 5% damping ratio, using the method proposed by Nigam and Jennings (1969). The response spectra obtained by manual processing in 35 tests performed were consistent with the response spectra contained in the database.

The interface catalog obtained from the strong motion database does not show a homogeneous distribution with depth. Most of the seismicity is located between 30- and 60-km depths, with a peak of concentration at 50-km depth. The earthquakes of $M_w < 5.0$ are concentrated between 30- and 70-km depths (Figures 1b and 1c). This low-magnitude seismicity bias at shallow depths is likely linked to the spatial disposition of the stations of the KiK-net that are constrained by the geometry of mainland Japan, which is located between 250 to 300 km west of the Japanese trench.

4. GMPE Model Selection

To select an adequate GMPE model for the interface seismicity of the Japan subduction, two different models have been tested over the interface ground motion database. The first model considered (Abrahamson et al., 2016) has been developed using a worldwide catalog. It considers nonlinear site amplification and differentiates the attenuation of sites located in the forearc from those located back of the volcanic arc. The second selected model (Zhao et al., 2006) has been mainly developed with records of Japanese earthquakes and considers a gradual increment of the ground motion with the focal depth, for earthquakes deeper than 15 km. The ground motions predicted by both of these models have been computed for each record of the database, using the provided metadata on station positions with respect to the volcanic arc, sites conditions, moment magnitude, epicentral depth, and distance to the rupture.

To evaluate the fit of the models to the ground motion database, the predicted ground motions were compared to the corresponding observed response spectra for peak ground acceleration (PGA) and three additional oscillator fundamental frequencies (10, 1.0, and 0.66 Hz). Then the total residuals, which correspond to the difference between the observed and the predicted ground motions normalized by the standard deviation of the model, were computed as shown in equation (2):

$$Z_T{}^{ij}(T) = \frac{\log\left[Sa_{obs}{}^{ij}(T)\right] - \log\left[Sa_{pred}{}^{ij}(T)\right]}{\sigma(T)} \tag{2}$$

where $Z_T{}^{ij}(T)$ is the total residual at site j for event i at oscillator period T, $Sa_{obs}{}^{ij}(T)$ and $Sa_{pred}{}^{ij}(T)$ correspond to the observed and predicted acceleration response spectra at site j for event i at oscillator period T, respectively, and $\sigma(T)$ is the total standard deviation of the model for oscillator period T.

Then, the total residuals have been disaggregated into between-event and within-event residuals using equations (3) and (4):

$$Z_B{}^{i}(T) = \frac{\tau(T) * \sum_{j=1}^{n} \left[\ \log\left[Sa_{obs}{}^{ij}(T)\right] - \mathrm{Log}\left[Sa_{pred}{}^{ij}(T)\right]\ \right]}{n * \tau(T)^2 + \phi(T)^2} \tag{3}$$

$$Z_W{}^{ij}(T) = \frac{\mathrm{Log}\left[Sa_{obs}{}^{ij}(T)\right] - \mathrm{Log}\left[Sa_{pred}{}^{ij}(T)\right] - Z_B{}^{i}(T) * \tau(T)}{\phi(T)} \tag{4}$$

where $Z_B{}^{i}(T)$ corresponds to the between-event residuals of the event i at oscillator period T, $Z_W{}^{ij}(T)$ corresponds to the within-event residuals of the event i at site j for oscillator period T, n corresponds to the number of records of the event i, and $\tau(T)$ and $\phi(T)$ are the standard deviations of the between-event and the within-event residuals, respectively, of the model at oscillator period T.

Finally, the dispersion of total, between-event, and within-event residuals has been compared with the dispersion of both selected models.

The within-event residuals represent the variation of the ground motions generated by a random variability of factors related with the spatial conditions between the site and the source, such as the travel path followed by the waves and site conditions. They are representative of the crustal structure complexity that cannot be captured by simple parameters such as distance to the source, site classification, or site shear wave velocity. On the other hand, the between-event residuals represent the variations of ground motions generated by random variability of source parameters not included in the predictive model. They reflect the variation of

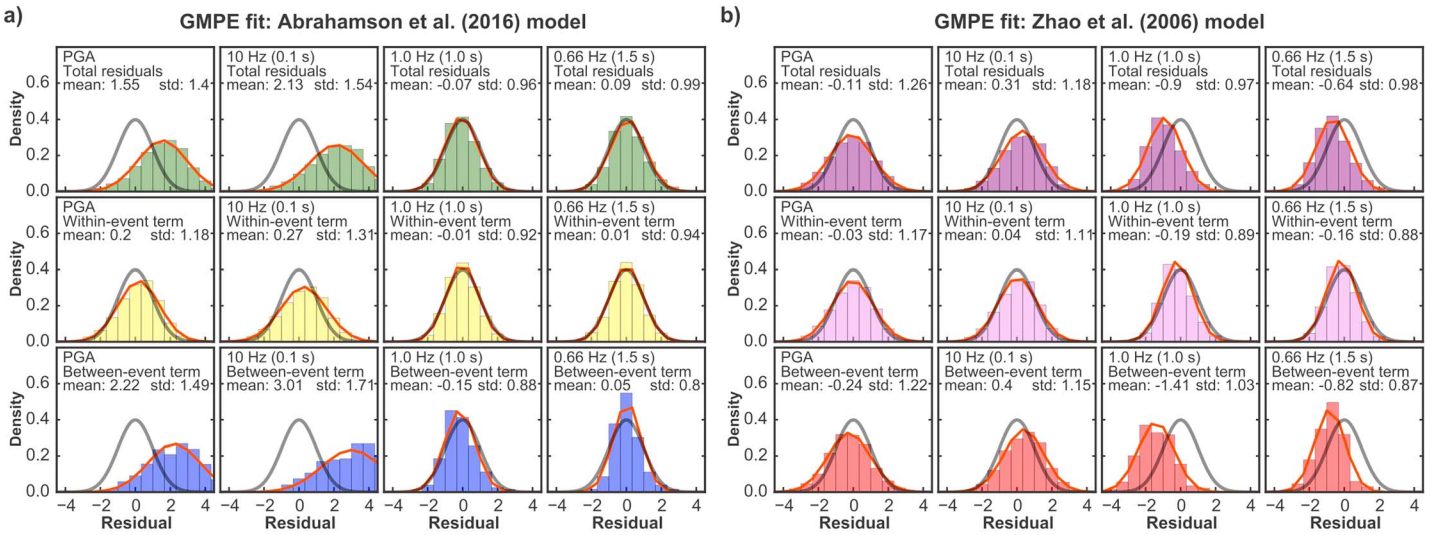

Figure 2. Histograms of ground motions residuals with respect to the ground motion prediction equation (GMPE) models tested. (a) Fit of the Abrahamson et al. (2016) model. (b) Fit of the Zhao et al. (2006) model fit. The black curves represent the normal density function of the model, and the red curve shows the normal density function of the data set residuals. The columns contain the residual distributions for peak ground acceleration and oscillator frequencies at 10, 1, and 0.66 Hz. The rows show from top to bottom the total, within-event, and between-event residuals, respectively.

source factors that cannot be captured by simple source parameters as the magnitude and the epicentral depth, such as the initial stress conditions, fluid pressure, stress drop, the slip distribution, slip velocity, rise time, rupture propagation, rupture velocity, or local fault damage (Al Atik et al., 2010; Baltay et al., 2017; Ktenidou et al., 2017; Strasser et al., 2009).

The total residual distribution shows that the model of Abrahamson et al. (2016) describes well the ground motion of our database for oscillators of low frequencies (1.0 and 0.66 Hz). It also captures well its variability. This is not the case at high frequencies (10 Hz and PGA), for which the standard deviation of the model is exceeded by the variability of the residuals and most of the ground motions are underestimated. The between-event residual distribution similarly shows a good fit for low frequencies and a poor fit for high frequencies (Figure 2a). It is important to note that a large part of database records have been generated by earthquakes of smaller magnitude ($M_w < 6$) than the earthquakes that have been used to calibrate the Abrahamson et al. (2016) model, which may explain those differences.

The residual standard deviation of the data set with respect to the Zhao et al. (2006) GMPE (Figure 2b) suggests that the model captures well the variability of the ground motions for all oscillator frequencies. The total residual distribution shows a good fit of the model to the ground motion data set at high frequencies, while the consistency decreases at low frequencies.

The total residual distribution of the Zhao et al. (2006) does not show any significant dependency on distance (supporting information Figure S1), and using the site residual term (Rodriguez-Marek et al., 2011) no particular site effects are detected on the stations of the KiK-network (Figure S2). Then, the fit between the within-event residual distribution indicates that the model reproduces well the variability associated with the site effects and path attenuations.

In the case of the Abrahamson et al. (2016) model, the dependency of the residuals on distance is significant (Figure S2). Additionally, a strong between-event residual dependency on magnitude and depth is also detected at high-frequency oscillators (Figure 3a). Despite this, it is possible to see that in the validity range of the model and for moment magnitudes higher than 6.0, the model predicts the ground motions adequately.

For the Zhao et al. (2006) GMPE model, the between-event residuals do not show obvious dependencies on magnitude at high oscillator frequencies, particularly for magnitudes higher than 4.5 (Figure 3b). Below this magnitude, a bias toward positive values of between-event residuals is detected. This bias may be an artifact generated by the limited number of records of low-magnitude earthquakes at shallow depths in the database. To test this hypothesis, the completeness magnitude of the catalog has been calculated for different

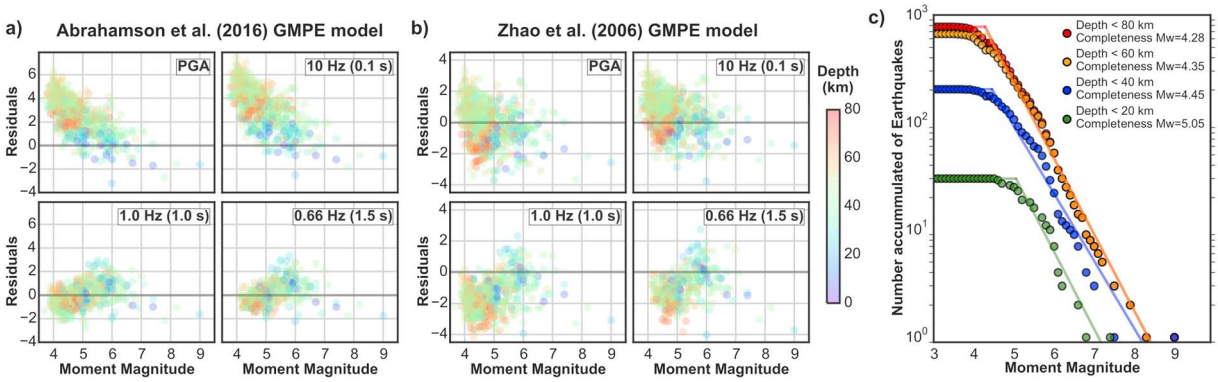

Figure 3. (a) Between-event residual distribution with respect to earthquake moment magnitude for Abrahamson et al. (2016) and (b) Zhao et al. (2006) ground motion prediction equations (GMPEs) model. The colors represent the depth of the epicenters. (c) Gutenberg-Richter law of the Dawood et al. (2016) subduction interface earthquakes as a function of the epicentral depth. Note the inversely proportional relation between the completeness magnitude and the cutoff depth, suggesting the progressive decrease of the KiK-net capability of getting good quality strong motion records for low M_w earthquakes toward the trench. PGA = peak ground acceleration.

depth ranges (Figure 3c). The results show that the completeness magnitude increases near the trench, which confirms a deficit of ground motion observations from low-magnitude shallow earthquakes.

These results show that only the Zhao et al. (2006) model is capable of describing the scaling and variation of ground motions on a large magnitude range. This makes this model the best suited to be used as a backbone to study the ground motion variations of the earthquakes contained in the database. Since the results described in the following sections are based on the between-event residuals of the Zhao et al. (2006) model, it is important to note that although the Abrahamson et al. (2016) model is less well suited to reproduce the variability of our data set, the relative spatial and temporal variability of its between-event residuals show similar patterns than for the Zhao et al. (2006) model. In other words, the results presented in the following sections of this paper are fully consistent whatever the backbone model used.

5. Depth and Regional Variability of Ground Motions and Lateral Variation of the Subduction Interface Properties

For the between-event residual being computed for all the earthquakes, their spatial distribution can be analyzed in order to identify regional features, following the approach from Piña-Valdés et al. (2018). Between-event residual patterns can therefore be used to map the variability of energy release. The identification of spatial variations of between-event residuals of earthquakes may highlight some ground motion dependencies that are currently missing in GMPE development. Also, such spatial variability may lead in a better description of the variability of fault interface characteristics, such as frictional and roughness properties that may impact the ground motions.

The distribution of between-event residuals in depth and in space has therefore been analyzed. If all residuals from the regions of Honshu and Hokkaido are analyzed together, the residuals show a slight decrease with depth at low frequencies (1.0 and 0.66 Hz), while no depth dependency of the between event residuals is visible at high oscillator frequencies (PGA and 10 Hz; Figure 4a). The fact that no significant depth dependency is seen in the residuals is actually expected since the GMPE model used as a backbone at high frequencies includes a correction for depth in its functional form (Zhao et al., 2006). Therefore, a null average dependency with depth of between event residuals means that the functional form of the Zhao et al. (2006) GMPE model mimics well the overall depth dependency of the interface earthquakes ground motions. It also implies that the deep earthquakes generate larger ground accelerations than the shallow ones.

When the spatial distribution of the between-event residuals is analyzed through a latitude-depth diagram (Figure 4b), a first-order dependency of the between-residuals on depth is, however, observable at high frequencies (PGA and 10 Hz) and is shown by the concentration of the highest values of the between-event residuals at depth. A finer spatial analysis reveals a lateral variability of the depth dependency of between-event

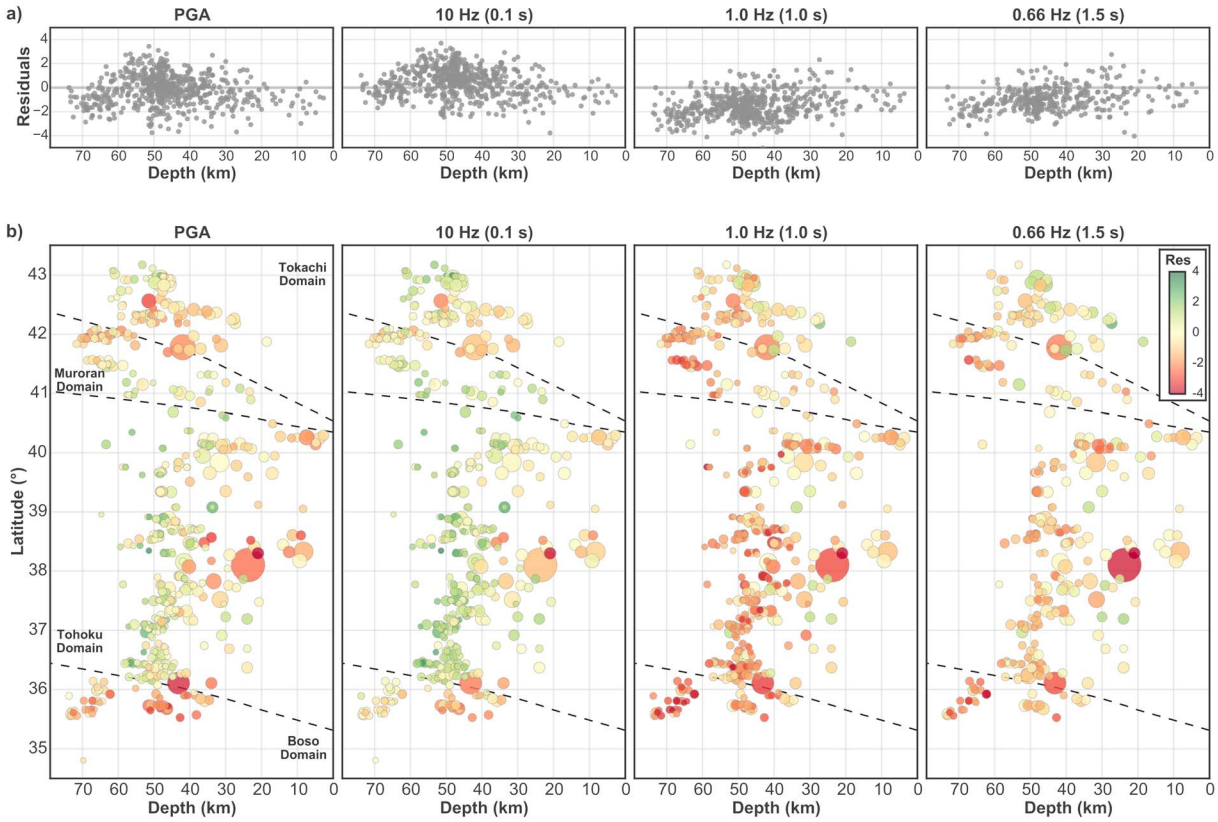

Figure 4. (a) Between-event residuals as a function of the epicentral depth at different oscillator frequencies (peak ground acceleration, PGA, 10, 1, and 0.66 Hz from left to right). (b) Between-event residuals of interface seismicity in a latitude-depth plot. The size of circles depends on the magnitude, and the colors represent the ground motion between-event residuals with respect to the Zhao et al. (2006) ground motion prediction equation model. The dashed lines represent imaginary boundaries perpendicular to the trench of four regions identified from depth distribution of the interface seismicity, the between-event residual variations, the geometry of the subducting slab, the strike of the trench, and the lateral variation of the main features of the free air gravity anomalies and interface geodetic coupling (see Figure 5). No significant depth dependency can be evidenced by examining the complete database as a whole, while a dependency with depth at high oscillator frequencies is seen from a domain to the other.

residuals and therefore ground motions. This indicates that the increase of ground shaking with depth at high frequencies can locally vary from the one embedded in the GMPE model of Zhao et al. (2006). Based on this observations and considering factors such as the spatial and depth distribution of the interface seismicity, the geometry of the subducting slab, the abrupt change of strike of the subduction trench, the lateral homogeneity of the free air gravity anomalies, and the main features of the geodetic coupling, four domains can be identified along the interface characterized by a different evolution of strong motions with epicentral depths (Figure 5a):

- Tokachi domain: located offshore Hokkaido, north of 42°N. Earthquakes in the database are concentrated between 40- and 60-km depths. In this region, the between-event residuals computed with respect to the Zhao et al. (2006) model present an increase with depth at high frequencies (PGA and 10 Hz).
- Muroran domain: located between 41°N and 42°N. It corresponds to a change in the trench orientation. Earthquakes in the database are located between 30- and 75-km depths. No obvious dependency of residuals with depth is observed.
- Tohoku domain: located between 36°N and 41°N. This portion of the subduction interface broke during the 2011 Tohoku-Oki M_w 9.0 earthquake. The database contains earthquakes that occurred between 10- and 60-km depths, thus shallower than in other portions of the Japan subduction. These earthquakes' between-event residuals increase with depth at high frequencies (PGA and 10 Hz).
- Boso domain: located south of 36°N offshore Boso. This portion of the Japan subduction is well known for the occurrence of regular slow slip earthquakes (Hirose et al., 2014; Ozawa, 2014; Ozawa et al., 2007;

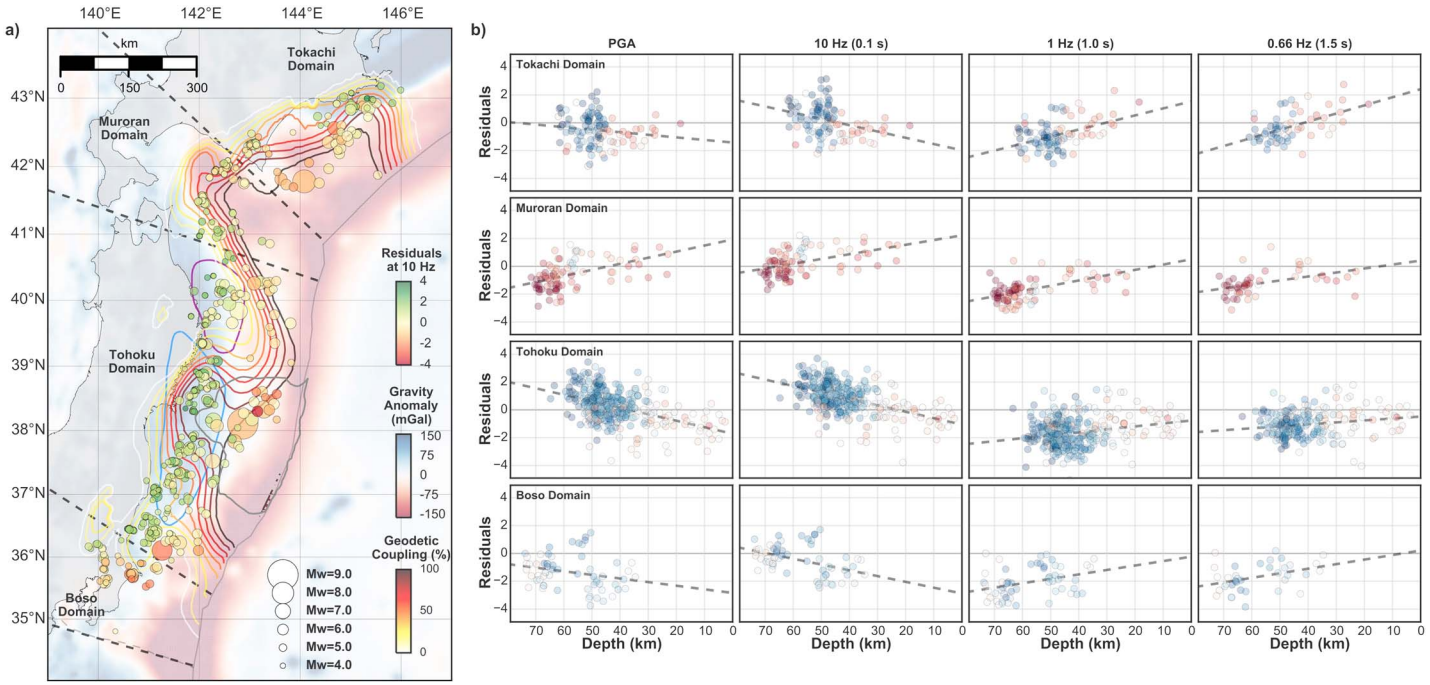

Figure 5. (a) Map of free air gravity anomaly derived from satellite altimetry on the Hokkaido and Honshu areas (Sandwell et al., 2013; Sandwell & Smith, 1997). The circles show the location of the interface seismicity, the size represents the moment magnitude, and the color represents the ground motion between-event residuals with respect to the Zhao et al. (2006) ground motion prediction equation (GMPE) model, for oscillator frequency of 10 Hz. The contour lines show the geodetic coupling (Φ) of the subduction interface, contoured each at $\Delta\Phi = 0.1$ (Loveless & Meade, 2011). The black dashed lines show the proposed lateral boundaries of the domains identified along the Japan megathrust. The purple and blue contours show the areas where 10-year transient decelerations and accelerations of interface slip have been observed before Tohoku-Oki earthquake (Mavrommatis et al., 2015). The gray contour shows the 10-m slip boundary of Tohoku-Oki earthquake (Hooper et al., 2013). (b) Distribution of ground motion between-event residuals with respect to Zhao et al. (2006) GMPE model as a function of the epicentral depth, for peak ground acceleration (PGA) and oscillator frequencies of 10, 1.0, and 0.66 Hz (from left to right). The colors represent the gravity anomaly at epicenters location. The four different domains are vertically sorted from north to south.

Reverso et al., 2016). The seismicity included in the database occurs between 30- and 75-km depths. Like for the Muroran domain, an increase of between-event residuals with depth is observed, although the number of earthquakes in the database is limited.

The distribution of the between-event residuals shows that depth affects the ground motions on a different manner from one domain to the other. This suggests a nonhomogeneous depth dependency of the frequency content of earthquakes that occurred on the Japan subduction interface. At high frequencies, the between-event residuals present a stronger depth dependency than the one considered by the Zhao et al. (2006) GMPE model for the Tokachi, Tohoku, and Boso domains (Figure 5b). It is also noticeable that the model overestimates most of the ground motions in the Boso domain.

6. Lateral Variability of the Japan Trench

The fact that each of the four domains identified shows its own distribution of between-event residuals with depth supports the idea of a lateral variability of the subduction interface mechanical properties.

In order to understand the meaning of these lateral variations and explore whether or not they could be persistent, the obtained distribution of between-event residuals is compared with independent geophysical markers such as the free air gravity anomaly (Sandwell et al., 2013; Sandwell & Smith, 1997) and the geodetic coupling in the region (Loveless & Meade, 2011; Figure 5a). The along-trench variability of the free air gravity anomalies derived from satellite altimetry helps in defining consistent lateral boundaries for the domains of the Japanese megathrust presented above. This is particularly striking in the area affected by the change of direction of the Japan Trench. Interseismic coupling derived from geodesy (Loveless & Meade, 2011) also shows a first-order correlation with the boundaries of the domains proposed above. Indeed, the domains

identified and their proposed boundaries are spatially correlated with geological, geometrical, and geographical markers, as well as with local features of the seismicity spatial distribution (e.g., the depth range of the seismicity epicenters varies from one identified domain to the other).

The Tokachi domain, located offshore of the north portion of the Hokkaido island at the northern end of the studied region, is a straight portion of the subduction where the Kuril Trench begins. No interface seismicity is registered in the database below 65-km depth. This portion of the subduction is characterized by a trench orientation that differs from the main portion of the Japan Trench, implying an oblique convergence of the Pacific Sea Plate at the trench, and with a slightly higher velocity than in the main portion of Japan Trench. This zone is associated at the north with a strong positive free air gravity anomaly below 45-km depth and a wide negative anomaly at shallower depths toward the trench. The southern part of this domain is affected by the subduction of the Erimo seamount that modifies locally the geometry of the subduction, which likely impacts the frictional behavior of the subduction interface (Cadet et al., 1987; Lallemand & Le Pichon, 1987). Here the geodetic seismic coupling is high, and a large negative free air gravity anomaly that reaches 75-km depth is also observed. Very low-frequency earthquakes have been detected in these regions during the seismic crisis of 2003 Tokachi-Oki earthquake (Asano et al., 2008; Obara et al., 2004), and the zone is characterized by large asperities that have broken in several opportunities in the last century (Hashimoto et al., 2009; Tanioka et al., 1997; Yagi, 2004).

The Muroran domain is located at the trench bend that separates two straight portions of the Japanese subduction characterized by different strike. In this area, the interface seismicity can reach 75-km depth (10 km deeper than in adjacent portions of the Japanese subduction). It is dominated by a large negative free air gravity anomaly, extending from the trench until a distance corresponding to 85-km depth of the slab interface, and shows a high geodetic coupling (Figure 5a).

The Tohoku domain corresponds to the portion of the Japan Trench offshore Honshu that ruptured during the 2011 Tohoku-Oki M_w 9.0 earthquake (e.g., Hooper et al., 2013; Kato et al., 2012; Simons et al., 2011; Yomogida et al., 2011). This domain is almost pure thrust, and its deeper portion (below 35-km depth) is characterized by a large positive free air gravity anomaly. Before the occurrence of the 2011 Tohoku-Oki megathrust, geodetic data have shown that the shallow portion of the interface was locked (Loveless & Meade, 2011; Suwa et al., 2006), while the deeper portion of the subduction interface has experimented a very long (~10 years) transient variation of slip rate and interseismic coupling (Loveless & Meade, 2016; Mavrommatis et al., 2015; Yokota & Koketsu, 2015). Interseismic coupling increased in the deep north portion of the interface, while it decreased in the central part, below the Tohoku-Oki rupture (i.e., slow acceleration of slip on the interface, associated with an increase in background seismicity; Marsan et al., 2017; Figure 5a, purple and blue contours, respectively). Similar to Tokachi domain, this lateral portion of the subduction interface does not present seismicity below 60-km depth.

Finally, the Boso domain, which is located at the southern limit of the Japan Trench offshore Boso, presents interface seismicity until 75-km depth, like the Muroran domain. This area is well known to host regular SSEs beneath the Boso peninsula with typical recurrence from 6 to 4 years and M_w around 6.5 (Ozawa et al., 2003, 2007). This area is characterized by the double subduction of the Philippine Sea Plate and of the Pacific Sea Plate below mainland Japan, making it difficult to separate interface earthquakes from others. This might explain the relative low number of interface earthquakes listed in the database. In this area it could therefore be worth to perform a finer analysis of the database earthquakes in order to perform a more complete classification of interface events and to identify whether these earthquakes belong to the Pacific plate slab or to the Philippine Sea plate slab.

7. Discussion

7.1. Validity of the GMPE Models Tested

The generation of a high-quality ground motion database requires the conjunction of two important ingredients: (1) a good and well-characterized seismological network able to provide proper records, and (2) a reliable earthquake catalog from which the metadata (magnitude, distance, and site conditions) can be extracted to document the ground motion records. In the case of Japan, the KiK-net provides high-quality earthquake acceleration records for one of the most active subduction zone of the world. Its large station

density and the high seismicity rate of the region have generated a valuable and unique collection of ground motion records for subduction earthquakes. In addition, the Japan Meteorological Agency provides a quite complete seismic catalog of the Japanese subduction zone. In this context, the automated processing of earthquake accelerations records proposed by Dawood et al. (2016) gave the opportunity to develop and disseminate a reliable interface earthquake's ground motion database, which cannot be obtained by manual processing due to the large quantity of information contained.

The results of the GMPE tests have shown that the Abrahamson et al. (2016) model correctly predicts the shaking resulting from large magnitude ($M_w \geq 6$) earthquakes at all frequencies tested (Figure 3a). For earthquakes of moderate and low magnitude ($4.0 \leq M_w \leq 6.0$) though, it only predicts proper values at low frequencies. The model of Zhao et al. (2006) has shown a good fit at all tested frequencies for magnitudes higher than 3.5.

The GMPE residual analysis is based on residual partitioning. This method has a meaning only if the GMPE model is not biased by a difference between the observed and predicted distance decay (Mak et al., 2018). Our analysis shows that the total residuals do not show significant dependency on rupture distance for the Zhao et al. (2006) GMPE model (Figure S1). Residual distance dependencies are much larger for the Abrahamson et al. (2016) model. These results favor the use of the Zhao et al. (2006) model to analyze and predict ground shaking of Japanese subduction earthquakes in a large magnitude range. However, it should be noted that the relative time and space variability of the between-event residuals is fully consistent from one reference GMPE to the other (Figures S3, S4, S5, S6, S7, S9, S11, and S13), pleading for the strength of our analysis.

7.2. Frictional Interpretation of the Ground Motion Variability and Link With the Interseismic Coupling

In order to check that the relative values of the between-event residuals have compatible results with those derived from classical Fourier spectral ratios used to analyze the event-to-event ground-motion variations, we searched in our data set pairs of earthquakes of similar magnitudes ($\Delta M_w \leq 0.1$) of M_w higher than 5.0, with distance to each other no larger than 25 km and with differences larger than 2 of between-event residuals at high frequencies (PGA and 10 Hz). Five pairs of earthquakes that fill those requirements were founded. We have computed the Fourier spectral ratios using the time histories available from stations of the KiK-net and K-net networks (Figure 6).

Since the Zhao et al. (2006) GMPE model only predicts the horizontal ground motions, the spectral ratios were computed from surface and borehole records, using the average horizontal Fourier spectra that have been obtained using equation (5):

$$F_{hor}(f) = \sqrt{F_{NS}(f)^2 + F_{EW}(f)^2} \tag{5}$$

where F_{NS} and F_{EW} correspond to the smoothed Fourier spectra of the north-south and east-west acceleration components, respectively, and F_{hor} to the horizontal Fourier spectra. One spectral ratio has been computed at each station for a single pair of earthquakes, then the spectral ratios of all stations have been averaged for each frequency f, using equation (6):

$$SR_{1-2}(f) = \sqrt[n]{\prod_{j=1}^{n} \frac{F_2^j(f)}{F_1^j(f)}} \tag{6}$$

where F_1^j and F_2^j are the horizontal Fourier spectra of events 1 and 2 at the station j and n is the number of stations that have recorded both events.

The spectral ratios obtained for all earthquake pairs confirm that the relative difference of the between-event residuals can be interpreted as changes in the earthquake frequency content of the ground motion records in the frequency band considered here (0.5–10 Hz). These results are consistent with recent tests conducted by Bindi et al. (2017) who have shown that the general trends observed in the Fourier domain (e.g., the between-event dependence on stress drop) are also observed for the response spectra even if, as expected from their definition, response spectra are smoothing the frequency-to-frequency variability of ground motions, in particular, at frequencies larger than 10 Hz. The theoretical dependencies between Fourier and Response spectra

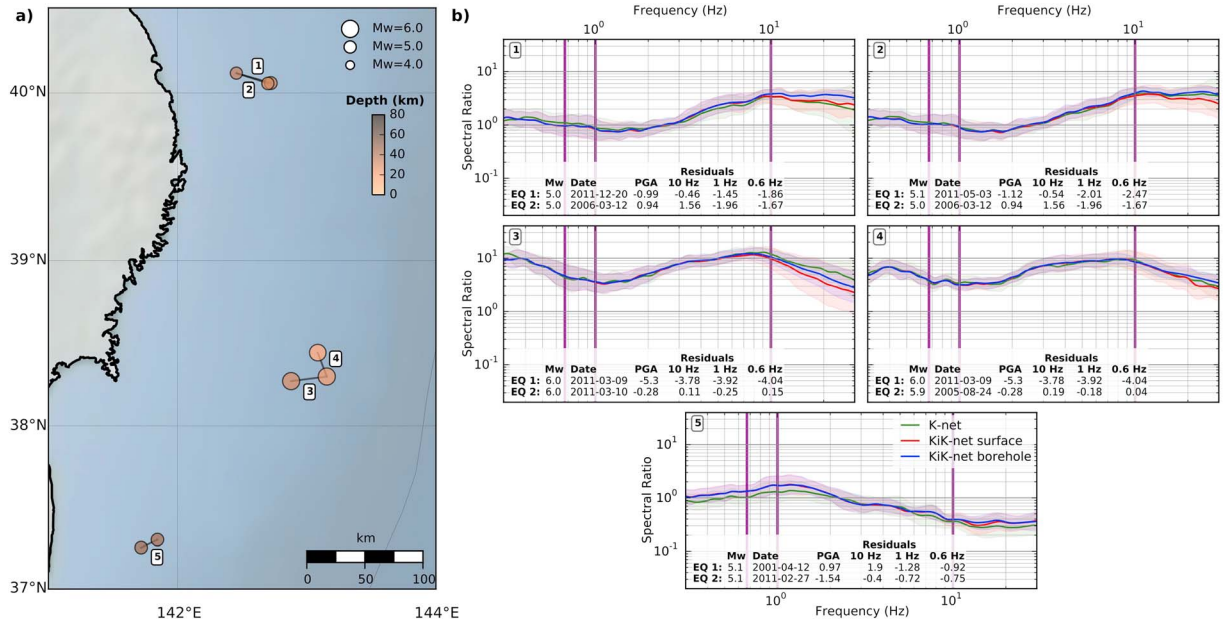

Figure 6. (a) Map with the location of pairs of earthquakes of similar magnitude, M_w higher than 5.0, distance to each other lower than 25 km, and between-event residual difference larger than 2. The numbers correspond to the pair identification. (b) Spectral ratios computed from surface and borehole records from the K-net and KiK-net networks stations using as reference on each pair the earthquake labeled as equation (1). Shaded regions show the spectral ratio standard deviation, and vertical purple lines correspond to the fundamental oscillator frequency at which the between-event residuals are informed. The spectral ratios show that the frequencies with values around 1 correspond to small differences in between-event residuals at a given oscillator frequency; meanwhile, large differences in between-event residuals are associated to spectral ratios far from 1. Note that the relative lower between-event residual values are systematically associated to lower amplitude on the earthquake frequency content at the corresponding frequencies. PGA = peak ground acceleration.

have been analyzed in detail by Bora et al. (2016). This study shows that the value of the response spectra at a given oscillator frequency is controlled not only by the amplitude of the Fourier spectra at that single frequency but by the contribution of the whole frequency content. However, for response spectral ordinates below the peak of response spectra, this value can be considered equivalent to the scaling of the Fourier spectral ordinates at the same frequencies. We then have been checking the peak of the response spectra of the data set used in this study (Figure S14): the peak, as expected is magnitude-dependent, and for the vast majority of earthquakes and stations, the peak is higher than 10 Hz (the response maximum frequency used to analyze time and regional dependencies).

The use of *S* wave Fourier spectra and the development of similar tests were, however, not possible because of the lack of GMPEs developed for Fourier spectra of subduction earthquakes and the fact that the Dawood et al. (2016) database was developed only for response spectra.

The measured between-event residuals show a regional dependency. The observed depth dependency of ground motions generated by interface earthquakes is consistent with the variability of the stress drop of Japanese earthquakes (Nakano et al., 2015), observed for events larger than 5.0 (Denolle & Shearer, 2016) as well as for small earthquakes of magnitudes between 3.5 and 4.0 (Uchide et al., 2014). Additionally, these findings are in agreement with variation of the energy radiation patterns observed during the 2011 Tohoku-Oki megathrust earthquake M_w 9.0 (Ide et al., 2011; Irikura & Kurahashi, 2011; Kiser & Ishii, 2012; Satriano et al., 2014) and with the downdip segmentation of the subduction interface proposed by Lay et al. (2012).

The Tokachi and Boso domains show a significant change of the between-event residual values at high frequencies (PGA and 10 Hz) around 50-km depth. For earthquakes located in the Tohoku domain, a depth dependency of the between-event residuals is also observed, but with a progressive change in values (Figure 5b). This may be interpreted as the transition between the shallow domain B and the deeper domain C proposed by Lay et al. (2012), which are characterized respectively by unstable slip regions hosting large patches strongly locked during the interseismic period and slipping largely during megathrust events, and

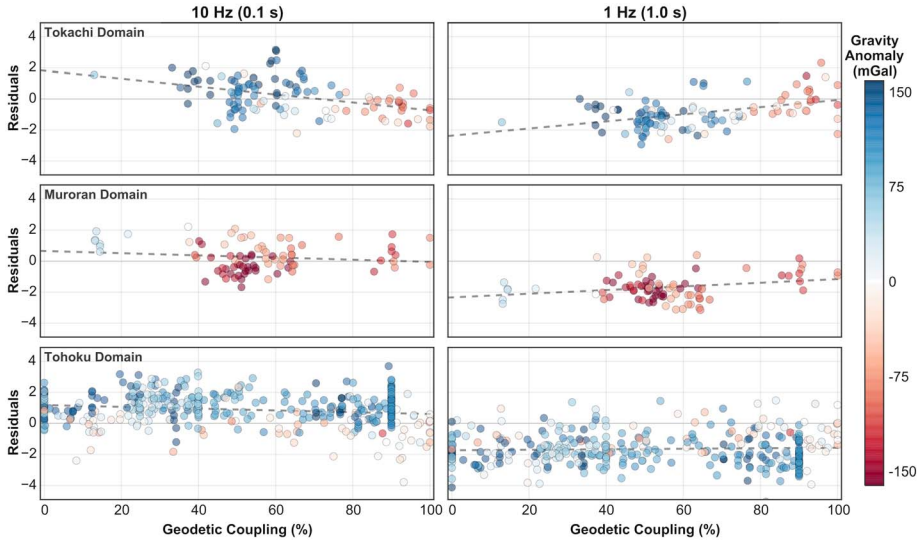

Figure 7. Variation of between-event residuals computed with respect to the Zhao et al. (2006) ground motion prediction equation versus geodetic interseismic coupling (Loveless & Meade, 2011), for oscillator frequencies of 10 and 1.0 Hz (left and right columns, respectively). The colors represent the free air gravity anomaly at epicenter locations (Sandwell et al., 2013; Sandwell & Smith, 1997). Boso domain has been excluded because of the little amount of data available in Dawood et al. (2016) database.

the metastable regions dominated by conditionally stable areas with medium-sized to small isolated asperities that radiate a large amount of high-frequency energy when they break.

The variability of the frictional properties of the subduction interface should impact the first-order pattern of interseismic coupling (Hetland & Simons, 2010; Kaneko et al., 2010). We can therefore expect a correlation between interseismic coupling and generated ground motions. Interseismic coupling has indeed been observed to decrease with depth on all subduction zones, in agreement with the depth dependency observed in the seismic energy release, and with depth-dependent frictional segmentation models (Lay et al., 2012). Our data set confirms this hypothesis: the distribution of the between-event residuals compares well with the geodetic coupling map (Figure 5a). The interface earthquakes that ruptured highly coupled areas generate radiation of lower amplitudes at high frequency than the earthquakes that occurred on poorly coupled areas on Tokachi and Muroran domains, where no major transient slip has been observed (Figure 7). The large energy release at high frequency may be produced by a rough surface (e.g., a group of small asperities) in the metastable region, which generates an average medium geodetic coupling and transient stress shadows (Hetland & Simons, 2010). Instead, large persistent asperities would generate smooth ruptures (i.e., low-energy release at high frequency) and a nearly full coupling.

7.3. Persistent Versus Transient Features and Temporal Variability of Ground Motions

The strongly negative free air gravity anomalies on subduction zones have been related with the increase of shear traction and associated to high coefficient of friction on the plate interface (Song & Simons, 2003). After these authors, these high shear tractions and friction coefficients would control the long-term seismic coupling of the subduction interface. The computed between-event residuals at high frequencies (10 Hz) seem to be spatially correlated with the geodetic coupling and the free air gravity anomaly; consistently with the depth-dependency observed (Figure 5a), the deeper portion of the subduction interface shows higher between-event residuals at high frequencies, lower geodetic coupling, and positive free air gravity anomalies. This correlation of the between-event residuals, geodetic coupling, and free air gravity anomaly is particularly clear in Tokachi and Muroran domains, while in the Tohoku domain no obvious correlation can be seen (Figure 7).

The Tohoku domain (Figure 8a), which has hosted Tohoku earthquake in 2011, has undergone a decade of geodetic coupling variation at depth and background seismicity rate variability, which indicates transient slip behavior (Loveless & Meade, 2016; Marsan et al., 2017; Mavrommatis et al., 2015; Yokota & Koketsu, 2015). The

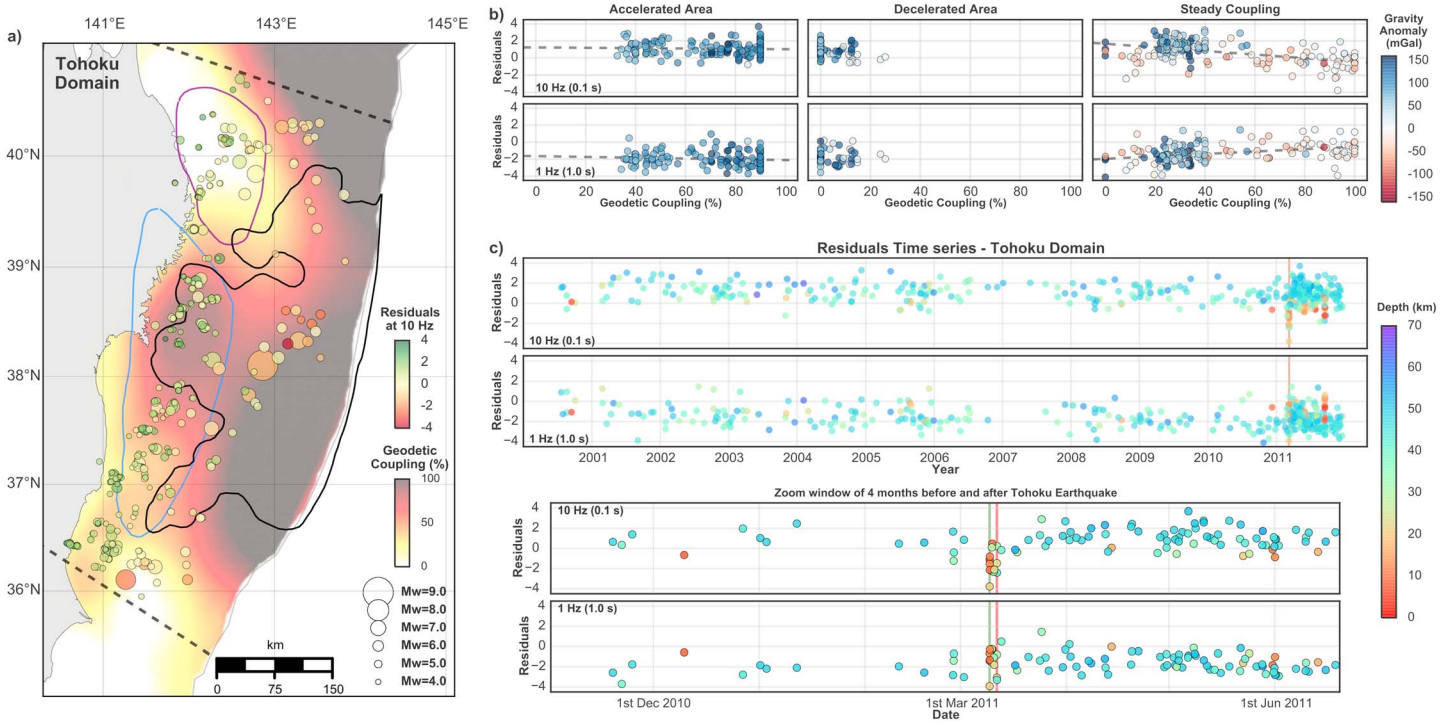

Figure 8. (a) Map of geodetic coupling of Tohoku domain (Loveless & Meade, 2011). The circles show the location of the interface seismicity, the size represents the moment magnitude, and the color represents the ground motion between-event residuals with respect to Zhao et al. (2006) ground motion prediction equation (GMPE) model for oscillator frequency of 10 Hz. The black dashed lines show the lateral boundaries of the domain. The purple and blue contours show the areas where transient deceleration and acceleration of interface slip have been observed respectively in the 10 years preceding the earthquake (Mavrommatis et al., 2015). The black contour shows the boundary of Tohoku-Oki earthquake rupture (Hooper et al., 2013). (b) Variation of between-event residuals with respect to Zhao et al. (2006) GMPE versus geodetic interseismic coupling, for oscillator frequencies of 10 and 1.0 Hz, separated by regions that have shown accelerated and decelerated transient slip and the region with a steady coupling during 10 years before Tohoku-Oki earthquake M_w 9. (c) Time series of the ground motion between-event residuals with respect to Zhao et al. (2006) GMPE model of whole Tohoku domain between 2000 and 2011 Tohoku-Oki earthquake M_w 9, for oscillator frequencies of 10 and 1.0 Hz. The vertical red line represents the Tohoku Oki mainshock, and the vertical green line represents the large M_w 7.3 earthquake that occurred on 9 March 2011.

geodetic coupling map (Figures 5 and 8) was derived from a GPS velocity field obtained from observations spanning the January 1997 to May 2000 period (Loveless & Meade, 2010), hence before the occurrence of the decadal transient slip observed on the interface (Mavrommatis et al., 2015; Yokota & Koketsu, 2015). The location of the deeper coupled patch on this geodetic coupling map corresponds to a region with a strong positive free air gravity anomaly that experienced a decadal transient slip behavior (Figure 5a). This suggests that this coupled area is not persistent over the long term but rather corresponds to a transient feature. We have therefore performed a detailed analysis of Tohoku domain, by separating it into three zones: the area where slip was accelerated before Tohoku (blue contour in Figures 5a and 8a), the area where coupling increased before Tohoku (purple contour in Figures 5a and 8a), and elsewhere (i.e., areas of Tohoku domain characterized by a constant geodetic coupling through the last decade). Consistently with the domains characterized by a steady coupling (Tokachi and Muroran), this partitioning shows that the between-event residuals on steady coupling areas of the Tohoku domain (called *steady coupling* in Figure 8b) correlate with the geodetic coupling and with free air gravity anomalies. Instead, no correlation is observed on areas that experienced a transient acceleration or deceleration of slip during the 10 years preceding Tohoku earthquake (blue and purple contours, respectively; Figure 8b).

These observations suggest that persistent frictional features of the subduction interface seem to be characterized by a positive correlation between the high-frequency energy radiations (i.e., between-event residual at PGA or 10 Hz), free air gravity anomaly, and interseismic slip rate on the plate interface (i.e., $V_p(1-\Phi)$, where V_p is the rate of plate convergence and Φ the interseismic coupling). Instead, areas that do not exhibit such correlations may undergo a transient phenomenon, such as an accelerated aseismic slip, which may

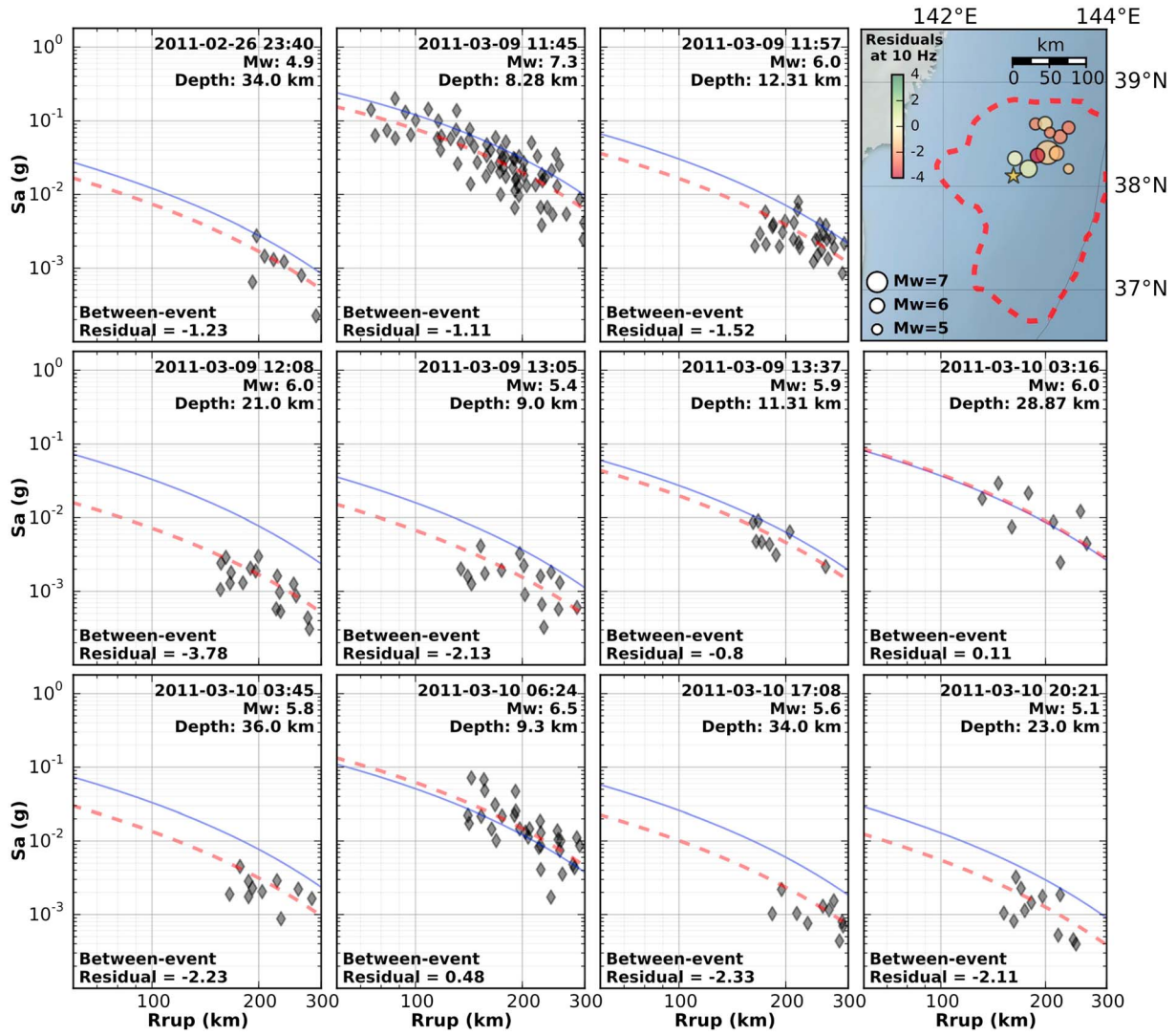

Figure 9. Comparison of the observed earthquake ground motions (gray diamonds) compared to the median ground motions predicted by the Zhao et al. (2006) ground motion prediction equation (blue solid line) and its correction by the between-event residual (red dashed line) for an oscillator frequency of 10 Hz, for earthquakes from the seismicity burst that preceded the Tohoku earthquake. The reference map shows with circles the epicenter location of the earthquakes, their size represents the magnitude, and their color the between-event residual for an oscillator frequency of 10 Hz. The yellow star shows the location of the epicenter of the Tohoku earthquake, and the dashed line shows the contour of the region that experienced a coseismic slip larger than 10 m (Hooper et al., 2013).

change the state of stress in nearby areas and potentially trigger a seismic rupture. In the areas affected by such transient behavior, the radiation of interface earthquake may be controlled by other mechanisms (Socquet et al., 2017), and its relationship with coupling or aseismic slip rate may differ significantly from the one observed in this study for stable areas.

To evaluate if transient slip behavior may impact the between-events residuals, we analyzed the temporal variability of the ground motions. Indeed, laboratory experiments have shown that a decrease on healing time reduced the high-frequency energy radiated (McLaskey et al., 2012). Time series of between-residuals have been analyzed for the Tohoku domain (Figure 8). The between-event residual time series do not show any obvious variation between 2000 and 2011 that would be associated with the 10-year change of slip rate on the subduction interface (Figure 8, bottom right). However, considering that the first earthquakes for which ground motion data are available in the database of Dawood et al. (2016) occurred in 2000, there are no good constraints on the state of the ground motions released by interface earthquake before the occurrence of the observed 10-year change of slip rate. A reference is therefore lacking, which would be needed to characterize the between-event residuals at the onset of the process. Despite this, an

anomalous drop of between-event residuals values is visible for a short time period on the time series at high frequencies (10 Hz), which is generated by earthquakes belonging to the sequence that preceded the M_w 9 Tohoku-Oki earthquake.

There are clear signs that preslip was occurring prior to the 2011 Tohoku-Oki earthquake, at the timescale of weeks: an increase in seismicity starting about 60 days before the mainshock (Ito et al., 2013; Kato et al., 2012; Marsan & Enescu, 2012), concurrent to an anomalous signal recorded by ocean-bottom pressure gauges (Ito et al., 2013), leads to the occurrence of a M_w 7.3 earthquake 3 days before the mainshock. This burst of seismicity is thought to reflect an ongoing aseismic slip on the subduction interface near the future hypocenter of the Tohoku-Oki mainshock. Also, it has been suggested recently that the burst of earthquake activity at shallow depths seen by these studies was also occurring at larger depth (>80 km), downdip the locked region of the subduction interface, based on intraslab earthquake rates and gravity variations (Bouchon et al., 2016). This activity could actually be the termination of the previously described much longer, slow decoupling process at intermediate depths, which could have started as early as 2003 (Mavrommatis et al., 2015; Yokota & Koketsu, 2015) or even years before according to seismicity rates (Marsan et al., 2017).

The ground motion database included only contains seven records that correspond to one earthquake (M_w 4.9) belonging to the first burst of seismicity that was recorded between 16 February and 2 March (Kato et al., 2016) and records of 10 earthquakes from the second seismicity burst, which started with the large interface earthquake of M_w 7.3 on 9 March and finished with the occurrence of the Tohoku-Oki earthquake M_w 9.0 (Figure 9). All of those earthquakes were distributed into a small area nearby the epicenter of Tohoku-Oki earthquake. This drop in energy release at high frequency is independent from the fact that these foreshocks are shallower than the background seismicity. Supporting information Figure S12 shows that the drop still exists when the data set is detrended from the dependency with depth. Instead, it is worth to note that during the weeks preceding Tohoku-Oki earthquake, the response spectra between-event residuals at 10 Hz drop below of the measures of central tendency of the whole data set. This is not observed anywhere else in the time series, even for aftershock sequences, such as the aftershocks following the Tohoku-Oki earthquake (Figure 8c). These observations suggest that the occurrence of a slow slip previous to the Tohoku-Oki rupture may have been generated by a progressive and fast degradation of the fault roughness before the large rupture of Tohoku-Oki earthquake. This could explain the drop of the high-frequency between-event residuals visible on the time series and the low ground motions observed for this group of earthquakes with respect to the predictions of the Zhao et al. (2006) GMPE model (Figure 9).

8. Conclusions

Under certain conditions taking into account the limitations of the response spectra compared to the Fourier spectra, GMPEs may be used for applications that go well beyond seismic hazard assessment. In particular, between-event residuals, which have been shown to be correlated with the stress drops (Bindi et al., 2007, 2017; Oth et al., 2017), can be spatially analyzed in order to identify variations of the frictional properties of large seismogenic faults (Piña-Valdés et al., 2018). The findings presented in this work are consistent with the downdip segmentation of the frictional properties on subduction interface proposed by Lay et al. (2012) and also with the main features of the frictional segmentation model proposed for Miyagi area by Satriano et al. (2014). This supports the use of the between-event residuals and ground motions generated by earthquakes as a proxy for the variability of the frictional properties of the subduction interface.

The ground motions generated by interface subduction earthquakes are regionally and depth dependent. Since the GMPEs are fundamental tools in the seismic hazard evaluation, the implementation of methodologies that allow minimizing the underestimation of the seismic hazard derived from the ground motion regional dependency is imperative. Variations in the earthquake ground motions from one region to another are expected. The calibration of GMPE models with large databases that include records from different regions can lead to an oversimplified estimation of the effects of parameters that represent the earthquake source. This could even be more important for earthquake records of low and moderate moment magnitude, which do not break the entire seismogenic zone, while for earthquakes of large magnitude, the effects of the regional variability of ground motion should impact less the prediction because these large earthquakes rupture a larger portion of the faults interfaces, therefore smoothing the spatial variability of strong motions.

The regional variability of ground motions, as well as the spatial distribution of the interface seismicity, the changes in the geometry of the Japan subduction interface, and the spatial distribution of geodetic coupling and free air gravity anomaly, shows an overall good agreement (Figure 5). This information has allowed to propose four individual lateral domains that control the generation of a specific signature in ground motions along the Japanese subduction interface, offshore Hokkaido, and Honshu regions, which show an internally consistent between-event residual distribution. The so-defined lateral domains are consistent with the strong free air gravity anomalies that can be interpreted as a proxy for the long-term slip behavior of subduction interface (Song & Simons, 2003). The lateral variation of between-event residual depth dependency may be related to the lateral variation of parameters that control the frictional behavior of the subduction interface such as temperature gradient, geometry, or fault normal stress, and they can drive to the variability of the downdip segmentation boundaries proposed by Lay et al. (2012).

The interseismic geodetic coupling maps can be interpreted as the result of an interfingering of seismic asperities and metastable regions, the highly coupled areas being rather constituted by large unstable seismic asperities fully locked between large earthquakes and the moderately coupled areas being made of small asperities whose stress shadows hinder the slip of surrounding metastable regions (Hetland & Simons, 2010). The inverted correlation between the observed strong radiations of high-frequency seismic energy (PGA and response spectra between-event residuals computed at 10 Hz) and the interseismic geodetic coupling corroborates this interpretation. Poorly coupled areas, constituted of an interfingering of small asperities and metastable areas, are characterized by a heterogeneous frictional behavior that likely complicates the seismic rupture and enhances the generation of high-frequency radiations. Instead, highly coupled areas are more homogeneous (large unstable seismic asperities) and would generate less high-frequency radiations.

It has been shown that strong free air gravity anomalies are related to the long-term features of subduction interface coupling (Song & Simons, 2003). The positive correlations observed between free air gravity anomalies, interseismic coupling, and ground motions tend to indicate persistent features of the interface. The analysis of between-event residual distribution cross-compared with other geophysical observables could therefore be a helpful method to identify persistent features on the seismogenic subduction interface. Instead, inconsistencies between the strong gravity anomalies, the geodetic coupling, and the signature of strong ground motions seem to occur in regions of the subduction interface affected by a transient behavior. Such inconsistencies may therefore be used as a proxy for the identification of such metastable areas affected by a transient slip behavior and to relate them with a potential enhanced seismic hazard updip. Finally, a drop of seismic energy released at high frequency can be observed for earthquakes belonging to the seismic sequence that preceded Tohoku-Oki M_w9 megathrust, similar to what has been observed off-shore Chile before the 2014 Iquique earthquake (Socquet et al., 2017).

Acknowledgments
This work has been supported by the BecasChile scholarship program by the Comisión Nacional de Ciencia y Tecnología de Chile (CONICYT) and by the Agence Nationale de la Recherche (ANR-17-CE31-0002-01) AtypicSSE project. We would like also to thank Yehuda Ben Zion and two anonymous reviewers for their constructive comments. We warmly thank Haisham Dawood and Adrian Rodrigues-Marek for making their database available (https://data-centerhub.org/resources/272). We are very grateful to the National Research Institute for Earth Science and Disaster Prevention (NIED), Japan, for providing the K-net and Kik-net data available on their web site (http://www.kyoshin.bosai.go.jp).

References

Abrahamson, N., Gregor, N., & Addo, K. (2016). BC Hydro ground motion prediction equations for subduction earthquakes. *Earthquake Spectra*, *32*(1), 23–44. https://doi.org/10.1193/051712EQS188MR

Abrahamson, N. A., & Youngs, R. R. (1992). A stable algorithm for regression analyses using the random effects model. *Bulletin of the Seismological Society of America*, *82*(1), 505–510.

Aki, K. (1967). Scaling law of seismic spectrum. *Journal of Geophysical Research*, *72*(4), 1217–1231. https://doi.org/10.1029/JZ072i004p01217

Aki, K. (1993). Local site effects on weak and strong ground motion. *Tectonophysics*, *218*(1–3), 93–111. https://doi.org/10.1016/0040-1951(93)90262-I

Akkar, S., Sandıkkaya, M. A., Şenyurt, M., Azari Sisi, A., Ay, B. Ö., Traversa, P., et al. (2014). Reference database for seismic ground-motion in Europe (RESORCE). *Bulletin of Earthquake Engineering*, *12*(1), 311–339. https://doi.org/10.1007/s10518-013-9506-8

Al Atik, L., Abrahamson, N., Bommer, J. J., Scherbaum, F., Cotton, F., & Kuehn, N. (2010). The variability of ground-motion prediction models and its components. *Seismological Research Letters*, *81*(5), 794–801. https://doi.org/10.1785/gssrl.81.5.794

Ando, M. (1975). Source mechanisms and tectonic significance of historical earthquakes along the Nankai trough, Japan. *Tectonophysics*, *27*(2), 119–140. https://doi.org/10.1016/0040-1951(75)90102-X

Aoi, S., Kunugi, T., & Fujiwara, H. (2004). Strong-motion seismograph network operated by NIED: K-NET and KiK-net. *Journal of Japan association for earthquake engineering*, *4*(3), 65–74. https://doi.org/10.5610/jaee.4.3_65

Archuleta, R. J., & Hartzell, S. H. (1981). Effects of fault finiteness on near-source ground motion. *Bulletin of the Seismological Society of America*, *71*(4), 939–957.

Asano, Y., Obara, K., & Ito, Y. (2008). Spatiotemporal distribution of very-low frequency earthquakes in Tokachi-oki near the junction of the Kuril and Japan trenches revealed by using array signal processing. *Earth, Planets and Space*, *60*(8), 871–875. https://doi.org/10.1186/BF03352839

Baltay, A. S., Hanks, T. C., & Abrahamson, N. A. (2017). Uncertainty, variability, and earthquake physics in ground-motion prediction equations. *Bulletin of the Seismological Society of America*, *107*(4), 1754–1772.

Béjar-Pizarro, M., Carrizo, D., Socquet, A., Armijo, R., Barrientos, S., Bondoux, F., et al. (2010). Asperities and barriers on the seismogenic zone in North Chile: State-of-the-art after the 2007 M_w 7.7 Tocopilla earthquake inferred by GPS and InSAR data. *Geophysical Journal International*, *183*(1), 390–406. https://doi.org/10.1111/j.1365-246X.2010.04748.x

Bindi, D., Parolai, S., Grosser, H., Milkereit, C., & Durukal, E. (2007). Empirical ground-motion prediction equations for northwestern Turkey using the aftershocks of the 1999 Kocaeli earthquake. *Geophysical Research Letters*, *34*, L08305. https://doi.org/10.1029/2007GL029222

Bindi, D., Spallarossa, D., & Pacor, F. (2017). Between-event and between-station variability observed in the Fourier and response spectra domains: Comparison with seismological models. *Geophysical Journal International*, *210*(2), 1092–1104. https://doi.org/10.1093/gji/ggx217

Bird, P. (2003). An updated digital model of plate boundaries. *Geochemistry, Geophysics, Geosystems*, *4*(3), 1027. https://doi.org/10.1029/2001GC000252

Boore, D. M. (1972). A note on the effect of simple topography on seismic SH waves. *Bulletin of the Seismological Society of America*, *62*(1), 275–284.

Boore, D. M., & Bommer, J. J. (2005). Processing of strong-motion accelerograms: Needs, options and consequences. *Soil Dynamics and Earthquake Engineering*, *25*(2), 93–115. https://doi.org/10.1016/j.soildyn.2004.10.007

Bora, S. S., Scherbaum, F., Kuehn, N., & Stafford, P. (2016). On the relationship between Fourier and response spectra: Implications for the adjustment of empirical ground-motion prediction equations (GMPEs). *Bulletin of the Seismological Society of America*, *106*(3), 1235–1253. https://doi.org/10.1785/0120150129

Bouchon, M., Marsan, D., Durand, V., Campillo, M., Perfettini, H., Madariaga, R., & Gardonio, B. (2016). Potential slab deformation and plunge prior to the Tohoku, Iquique and Maule earthquakes. *Nature Geoscience*, *9*(5), 380–383. https://doi.org/10.1038/ngeo2701

Bouchon, M., Schultz, C. A., & Toksöz, M. N. (1996). Effect of three-dimensional topography on seismic motion. *Journal of Geophysical Research*, *101*(B3), 5835–5846. https://doi.org/10.1029/95JB02629

Byrne, D. E., Davis, D. M., & Sykes, L. R. (1988). Loci and maximum size of thrust earthquakes and the mechanics of the shallow region of subduction zones. *Tectonics*, *7*(4), 833–857. https://doi.org/10.1029/TC007i004p00833

Cadet, J.-P., Kobayashi, K., Aubouin, J., Boulègue, J., Deplus, C., Dubois, J., et al. (1987). The Japan trench and its juncture with the Kuril trench: Cruise results of the Kaiko project, Leg 3. *Earth and Planetary Science Letters*, *83*(1–4), 267–284. https://doi.org/10.1016/0012-821X(87)90071-9

Causse, M., & Song, S. G. (2015). Are stress drop and rupture velocity of earthquakes independent? Insight from observed ground motion variability. *Geophysical Research Letters*, *42*, 7383–7389. https://doi.org/10.1002/2015GL064793

Cotton, F., Archuleta, R., & Causse, M. (2013). What is sigma of the stress drop? *Seismological Research Letters*, *84*(1), 42–48. https://doi.org/10.1785/0220120087

Courboulex, F., Vallée, M., Causse, M., & Chounet, A. (2016). Stress-drop variability of shallow earthquakes extracted from a global database of source time functions. *Seismological Research Letters*, *87*(4), 912–918. https://doi.org/10.1785/0220150283

Cummins, P. R., Baba, T., Kodaira, S., & Kaneda, Y. (2002). The 1946 Nankai earthquake and segmentation of the Nankai trough. *Physics of the Earth and Planetary Interiors*, *132*(1-3), 75–87. https://doi.org/10.1016/S0031-9201(02)00045-6

Dawood, H. M., Rodriguez-Marek, A., Bayless, J., Goulet, C. A., & Thompson, E. (2016). A flatfile for the KiK-net database processed using an automated protocol. *Earthquake Spectra*, *32*(2), 1281–1302. https://doi.org/10.1193/071214EQS106

DeMets, C. (1992). Oblique convergence and deformation along the Kuril and Japan trenches. *Journal of Geophysical Research*, *97*(B12), 17,615–17,625. https://doi.org/10.1029/92JB01306

DeMets, C., Gordon, R. G., Argus, D., & Stein, S. (1990). Current plate motions. *Geophysical Journal International*, *101*(2), 425–478. https://doi.org/10.1111/j.1365-246X.1990.tb06579.x

Denolle, M. A., & Shearer, P. M. (2016). New perspectives on self-similarity for shallow thrust earthquakes. *Journal of Geophysical Research: Solid Earth*, *121*, 6533–6565. https://doi.org/10.1002/2016JB013105

Fujiwara, H., Aoi, S., Kunugi, T., & Adachi, S. (2004). Strong-motion observation networks of NIED: K-NET and KiK-Net. *Cosmos Report*.

Hashimoto, C., Noda, A., Sagiya, T., & Matsu'ura, M. (2009). Interplate seismogenic zones along the Kuril–Japan trench inferred from GPS data inversion. *Nature Geoscience*, *2*(2), 141–144. https://doi.org/10.1038/ngeo421

Hetland, E., & Simons, M. (2010). Post-seismic and interseismic fault creep II: Transient creep and interseismic stress shadows on megathrusts. *Geophysical Journal International*, *181*(1), 99–112. https://doi.org/10.1111/j.1365-246X.2009.04482.x

Heuret, A., Lallemand, S., Funiciello, F., Piromallo, C., & Faccenna, C. (2011). Physical characteristics of subduction interface type seismogenic zones revisited. *Geochemistry, Geophysics, Geosystems*, *12*, Q01004. https://doi.org/10.1029/2010GC003230

Hirose, H., Matsuzawa, T., Kimura, T., & Kimura, H. (2014). The Boso slow slip events in 2007 and 2011 as a driving process for the accompanying earthquake swarm. *Geophysical Research Letters*, *41*, 2778–2785. https://doi.org/10.1002/2014GL059791

Hooper, A., Pietrzak, J., Simons, W., Cui, H., Riva, R., Naeije, M., et al. (2013). Importance of horizontal seafloor motion on tsunami height for the 2011 M_w = 9.0 Tohoku-Oki earthquake. *Earth and Planetary Science Letters*, *361*, 469–479. https://doi.org/10.1016/j.epsl.2012.11.013

Hyndman, R. D., & Wang, K. (1993). Thermal constraints on the zone of major thrust earthquake failure: The Cascadia subduction zone. *Journal of Geophysical Research*, *98*(B2), 2039–2060. https://doi.org/10.1029/92JB02279

Hyndman, R. D., Yamano, M., & Oleskevich, D. A. (1997). The seismogenic zone of subduction thrust faults. *Island Arc*, *6*(3), 244–260. https://doi.org/10.1111/j.1440-1738.1997.tb00175.x

Ide, S., Baltay, A., & Beroza, G. C. (2011). Shallow dynamic overshoot and energetic deep rupture in the 2011 M_w 9.0 Tohoku-Oki earthquake. *Science*, *332*(6036), 1426–1429. https://doi.org/10.1126/science.1207020

Irikura, K., & Kurahashi, S. (2011). *Strong ground motions during the 2011 Pacific Coast off Tohoku, Japan earthquake*. Paper presented at the Proc. of the International Symposium on Engineering Lessons Learned from the.

Ito, Y., Hino, R., Kido, M., Fujimoto, H., Osada, Y., Inazu, D., et al. (2013). Episodic slow slip events in the Japan subduction zone before the 2011 Tohoku-Oki earthquake. *Tectonophysics*, *600*, 14–26. https://doi.org/10.1016/j.tecto.2012.08.022

Ito, Y., Obara, K., Shiomi, K., Sekine, S., & Hirose, H. (2007). Slow earthquakes coincident with episodic tremors and slow slip events. *Science*, *315*(5811), 503–506. https://doi.org/10.1126/science.1134454

Jara-Munoz, J., Melnick, D., Brill, D., & Strecker, M. R. (2015). Segmentation of the 2010 Maule Chile earthquake rupture from a joint analysis of uplifted marine terraces and seismic-cycle deformation patterns. *Quaternary Science Reviews*, *113*, 171–192. https://doi.org/10.1016/j.quascirev.2015.01.005

Kaneko, Y., Avouac, J.-P., & Lapusta, N. (2010). Towards inferring earthquake patterns from geodetic observations of interseismic coupling. *Nature Geoscience*, *3*(5), 363–369. https://doi.org/10.1038/ngeo843

Kato, A., Fukuda, J. i., Kumazawa, T., & Nakagawa, S. (2016). Accelerated nucleation of the 2014 Iquique, Chile M_w 8.2 earthquake. *Scientific Reports*, *6*(1). https://doi.org/10.1038/srep24792

Kato, A., Obara, K., Igarashi, T., Tsuruoka, H., Nakagawa, S., & Hirata, N. (2012). Propagation of slow slip leading up to the 2011 M_w 9.0 Tohoku-Oki earthquake. *Science*, *335*(6069), 705–708. https://doi.org/10.1126/science.1215141

Kiser, E., & Ishii, M. (2012). The March 11, 2011 Tohoku-Oki earthquake and cascading failure of the plate interface. *Geophysical Research Letters*, *39*, L00G25. https://doi.org/10.1029/2012GL051170

Kodaira, S., Hori, T., Ito, A., Miura, S., Fujie, G., Park, J. O., et al. (2006). A cause of rupture segmentation and synchronization in the Nankai trough revealed by seismic imaging and numerical simulation. *Journal of Geophysical Research*, *111*, B09301. https://doi.org/10.1029/2005JB004030

Kodaira, S., Kurashimo, E., Park, J.-O., Takahashi, N., Nakanishi, A., Miura, S., et al. (2002). Structural factors controlling the rupture process of a megathrust earthquake at the Nankai trough seismogenic zone. *Geophysical Journal International*, *149*(3), 815–835. https://doi.org/10.1046/j.1365-246X.2002.01691.x

Koper, K. D., Hutko, A. R., Lay, T., Ammon, C. J., & Kanamori, H. (2011). Frequency-dependent rupture process of the 2011 M_w 9.0 Tohoku earthquake: Comparison of short-period *P* wave backprojection images and broadband seismic rupture models. *Earth, Planets and Space*, *63*(7), 599–602. https://doi.org/10.5047/eps.2011.05.026

Koper, K. D., Hutko, A. R., Lay, T., & Sufri, O. (2012). Imaging short-period seismic radiation from the 27 February 2010 Chile (M_w 8.8) earthquake by back-projection of P, PP, and PKIKP waves. *Journal of Geophysical Research*, *117*, B02308. https://doi.org/10.1029/2011JB008576

Ktenidou, O.-J., Roumelioti, Z., Abrahamson, N., Cotton, F., Pitilakis, K., & Hollender, F. (2017). Understanding single-station ground motion variability and uncertainty (sigma): Lessons learnt from EUROSEISTEST. *Bulletin of Earthquake Engineering*, 1–26.

Lallemand, S., & Le Pichon, X. (1987). Coulomb wedge model applied to the subduction of seamounts in the Japan trench. *Geology*, *15*(11), 1065–1069. https://doi.org/10.1130/0091-7613(1987)15<1065:CWMATT>2.0.CO;2

Lay, T., & Bilek, S. (2007). Anomalous earthquake ruptures at shallow depths on subduction zone megathrusts. In *The seismogenic zone of subduction thrust faults* (pp. 476–511). New York: Columbia University Press.

Lay, T., Kanamori, H., Ammon, C. J., Koper, K. D., Hutko, A. R., Ye, L., et al. (2012). Depth-varying rupture properties of subduction zone megathrust faults. *Journal of Geophysical Research*, *117*, B04311. https://doi.org/10.1029/2011JB009133

Loveless, J. P., & Meade, B. J. (2010). Geodetic imaging of plate motions, slip rates, and partitioning of deformation in Japan. *Journal of Geophysical Research*, *115*, B02410. https://doi.org/10.1029/2008JB006248

Loveless, J. P., & Meade, B. J. (2011). Spatial correlation of interseismic coupling and coseismic rupture extent of the 2011 M_W = 9.0 Tohoku-Oki earthquake. *Geophysical Research Letters*, *38*, L17306. https://doi.org/10.1029/2011GL048561

Loveless, J. P., & Meade, B. J. (2016). Two decades of spatiotemporal variations in subduction zone coupling offshore Japan. *Earth and Planetary Science Letters*, *436*, 19–30. https://doi.org/10.1016/j.epsl.2015.12.033

Mak, S., Cotton, F., Gerstenberger, M., & Schorlemmer, D. (2018). An evaluation of the applicability of NGA-West2 ground-motion models for Japan and New Zealand. *Bulletin of the Seismological Society of America*, *2*(108), 836–856. https://doi.org/10.1785/0120170146

Marone, C. (1998). The effect of loading rate on static friction and the rate of fault healing during the earthquake cycle. *Nature*, *391*(6662), 69.

Marone, C., & Scholz, C. (1988). The depth of seismic faulting and the upper transition from stable to unstable slip regimes. *Geophysical Research Letters*, *15*(6), 621–624. https://doi.org/10.1029/GL015i006p00621

Marsan, D., Bouchon, M., Gardonio, B., Perfettini, H., Socquet, A., & Enescu, B. (2017). Change in seismicity along the Japan trench, 1990–2011, and its relationship with seismic coupling. *Journal of Geophysical Research: Solid Earth*, *122*, 4645–4659. https://doi.org/10.1002/2016JB013715

Marsan, D., & Enescu, B. (2012). Modeling the foreshock sequence prior to the 2011, M_w9. 0 Tohoku, Japan, earthquake. *Journal of Geophysical Research*, *117*, B06316. https://doi.org/10.1029/2011JB009039

Mavrommatis, A. P., Segall, P., Uchida, N., & Johnson, K. M. (2015). Long-term acceleration of aseismic slip preceding the M_w 9 Tohoku-Oki earthquake: Constraints from repeating earthquakes. *Geophysical Research Letters*, *42*, 9717–9725. https://doi.org/10.1002/2015GL066069

McLaskey, G. C., Thomas, A. M., Glaser, S. D., & Nadeau, R. M. (2012). Fault healing promotes high-frequency earthquakes in laboratory experiments and on natural faults. *Nature*, *491*(7422), 101–104. https://doi.org/10.1038/nature11512

Moreno, M., Melnick, D., Rosenau, M., Baez, J., Klotz, J., Oncken, O., et al. (2012). Toward understanding tectonic control on the M_w 8.8 2010 Maule Chile earthquake. *Earth and Planetary Science Letters*, *321*, 152–165.

Nakano, K., Matsushima, S., & Kawase, H. (2015). Statistical properties of strong ground motions from the generalized spectral inversion of data observed by K-NET, KiK-net, and the JMA Shindokei network in Japan. *Bulletin of the Seismological Society of America*, *105*(5), 2662–2680. https://doi.org/10.1785/0120140349

Nigam, N. C., & Jennings, P. C. (1969). Calculation of response spectra from strong-motion earthquake records. *Bulletin of the Seismological Society of America*, *59*(2), 909–922.

Obara, K. (2002). Nonvolcanic deep tremor associated with subduction in southwest Japan. *Science*, *296*(5573), 1679–1681. https://doi.org/10.1126/science.1070378

Obara, K., Haryu, Y., Ito, Y., & Shiomi, K. (2004). Low frequency events occurred during the sequence of aftershock activity of the 2003 Tokachi-Oki earthquake; A dynamic process of the tectonic erosion by subducted seamount. *Earth, Planets and Space*, *56*(3), 347–351. https://doi.org/10.1186/BF03353063

Oth, A., Miyake, H., & Bindi, D. (2017). On the relation of earthquake stress drop and ground motion variability. *Journal of Geophysical Research: Solid Earth*, *122*, 5474–5492. https://doi.org/10.1002/2017JB014026

Ozawa, S. (2014). Shortening of recurrence interval of Boso slow slip events in Japan. *Geophysical Research Letters*, *41*, 2762–2768. https://doi.org/10.1002/2014GL060072

Ozawa, S., Miyazaki, S., Hatanaka, Y., Imakiire, T., Kaidzu, M., & Murakami, M. (2003). Characteristic silent earthquakes in the eastern part of the Boso peninsula, Central Japan. *Geophysical Research Letters*, *30*(6), 1283. https://doi.org/10.1029/2002GL016665

Ozawa, S., Suito, H., & Tobita, M. (2007). Occurrence of quasi-periodic slow-slip off the east coast of the Boso peninsula, Central Japan. *Earth, Planets and Space*, *59*(12), 1241–1245. https://doi.org/10.1186/BF03352072

Piña-Valdés, J., Socquet, A., Cotton, F., & Specht, S. (2018). Spatiotemporal variations of ground motion in northern Chile before and after the 2014 M_w 8.1 Iquique megathrust event. *Bulletin of the Seismological Society of America*, *108*(2), 801–814. https://doi.org/10.1785/0120170052

Reverso, T., Marsan, D., Helmstetter, A., & Enescu, B. (2016). Background seismicity in Boso Peninsula, Japan: Long-term acceleration, and relationship with slow slip events. *Geophysical Research Letters*, *43*, 5671–5679. https://doi.org/10.1002/2016GL068524

Rodriguez-Marek, A., Montalva, G. A., Cotton, F., & Bonilla, F. (2011). Analysis of single-station standard deviation using the KiK-net data. *Bulletin of the Seismological Society of America*, *101*(3), 1242–1258. https://doi.org/10.1785/0120100252

Sanchez-Sesma, F. J. (1987). Site effects on strong ground motion. *Soil Dynamics and Earthquake Engineering*, *6*(2), 124–132. https://doi.org/10.1016/0267-7261(87)90022-4

Sandwell, D., Garcia, E., Soofi, K., Wessel, P., Chandler, M., & Smith, W. H. (2013). Toward 1-mGal accuracy in global marine gravity from CryoSat-2, Envisat, and Jason-1. *The Leading Edge*, *32*(8), 892–899. https://doi.org/10.1190/tle32080892.1

Sandwell, D. T., & Smith, W. H. (1997). Marine gravity anomaly from Geosat and ERS 1 satellite altimetry. *Journal of Geophysical Research*, *102*(B5), 10,039–10,054. https://doi.org/10.1029/96JB03223

Satriano, C., Dionicio, V., Miyake, H., Uchida, N., Vilotte, J.-P., & Bernard, P. (2014). Structural and thermal control of seismic activity and megathrust rupture dynamics in subduction zones: Lessons from the M_w 9.0, 2011 Tohoku earthquake. *Earth and Planetary Science Letters*, *403*, 287–298. https://doi.org/10.1016/j.epsl.2014.06.037

Scholz, C. H. (1998). Earthquakes and friction laws. *Nature*, *391*(6662), 37–42. https://doi.org/10.1038/34097

Simons, M., Minson, S. E., Sladen, A., Ortega, F., Jiang, J., Owen, S. E., et al. (2011). The 2011 magnitude 9.0 Tohoku-Oki earthquake: Mosaicking the megathrust from seconds to centuries. *Science*, *332*(6036), 1421–1425. https://doi.org/10.1126/science.1206731

Socquet, A., Piña-Valdes, J., Jara, J., Cotton, F., Walpersdorf, A., Cotte, N., et al. (2017). An 8 month slow slip event triggers progressive nucleation of the 2014 Chile megathrust. *Geophysical Research Letters*, *44*, 4046–4053. https://doi.org/10.1002/2017GL073023

Somerville, P. G. (2003). Magnitude scaling of the near fault rupture directivity pulse. *Physics of the Earth and Planetary Interiors*, *137*(1-4), 201–212. https://doi.org/10.1016/S0031-9201(03)00015-3

Song, T.-R. A., & Simons, M. (2003). Large trench-parallel gravity variations predict seismogenic behavior in subduction zones. *Science*, *301*(5633), 630–633. https://doi.org/10.1126/science.1085557

Strasser, F. O., Abrahamson, N. A., & Bommer, J. J. (2009). Sigma: Issues, insights, and challenges. *Seismological Research Letters*, *80*(1), 40–56. https://doi.org/10.1785/gssrl.80.1.40

Suwa, Y., Miura, S., Hasegawa, A., Sato, T., & Tachibana, K. (2006). Interplate coupling beneath NE Japan inferred from three-dimensional displacement field. *Journal of Geophysical Research*, *111*, B04402. https://doi.org/10.1029/2004JB003203

Tanioka, Y., Ruff, L., & Satake, K. (1997). What controls the lateral variation of large earthquake occurrence along the Japan trench? *Island Arc*, *6*(3), 261–266. https://doi.org/10.1111/j.1440-1738.1997.tb00176.x

Uchide, T., Shearer, P. M., & Imanishi, K. (2014). Stress drop variations among small earthquakes before the 2011 Tohoku-Oki, Japan, earthquake and implications for the main shock. *Journal of Geophysical Research: Solid Earth*, *119*, 7164–7174. https://doi.org/10.1002/2014JB010943

Wang, K., & Bilek, S. L. (2011). Do subducting seamounts generate or stop large earthquakes? *Geology*, *39*(9), 819–822. https://doi.org/10.1130/G31856.1

Wang, K., & He, J. (2008). Effects of frictional behavior and geometry of subduction fault on coseismic seafloor deformation. *Bulletin of the Seismological Society of America*, *98*(2), 571–579. https://doi.org/10.1785/0120070097

Wells, R. E., Blakely, R. J., Sugiyama, Y., Scholl, D. W., & Dinterman, P. A. (2003). Basin-centered asperities in great subduction zone earthquakes: A link between slip, subsidence, and subduction erosion? *Journal of Geophysical Research*, *108*(B10), 2507. https://doi.org/10.1029/2002JB002072

Yagi, Y. (2004). Source rupture process of the 2003 Tokachi-Oki earthquake determined by joint inversion of teleseismic body wave and strong ground motion data. *Earth, Planets and Space*, *56*(3), 311–316. https://doi.org/10.1186/BF03353057

Yamanaka, Y., & Kikuchi, M. (2004). Asperity map along the subduction zone in northeastern Japan inferred from regional seismic data. *Journal of Geophysical Research*, *109*, B07307. https://doi.org/10.1029/2003JB002683

Yokota, Y., & Koketsu, K. (2015). A very long-term transient event preceding the 2011 Tohoku earthquake. *Nature Communications*, *6*(1). https://doi.org/10.1038/ncomms6934

Yomogida, K., Yoshizawa, K., Koyama, J., & Tsuzuki, M. (2011). Along-dip segmentation of the 2011 off the Pacific coast of Tohoku earthquake and comparison with other megathrust earthquakes. *Earth, Planets and Space*, *63*(7), 34.

Zhao, J. X., Zhang, J., Asano, A., Ohno, Y., Oouchi, T., Takahashi, T., et al. (2006). Attenuation relations of strong ground motion in Japan using site classification based on predominant period. *Bulletin of the Seismological Society of America*, *96*(3), 898–913. https://doi.org/10.1785/0120050122